



1 **Controls on spatial and temporal variability of streamflow**  
2 **and hydrochemistry in a glacierized catchment**

3 **Running title: Controls on streamflow and hydrochemistry in a glacierized catchment**

4 Michael Engel<sup>1</sup>, Daniele Penna<sup>2</sup>, Giacomo Bertoldi<sup>3</sup>, Gianluca Vignoli<sup>4</sup>, Werner Tirler<sup>5</sup>, and  
5 Francesco Comiti<sup>1</sup>

6 <sup>1</sup>Faculty of Science and Technology, Free University of Bozen-Bolzano, Piazza Università 5,  
7 39100 Bozen-Bolzano, Italy

8 <sup>2</sup>Department of Agricultural, Food and Forestry Systems, Via S. Bonaventura, 13, University  
9 of Florence, 50145 Florence, Italy

10 <sup>3</sup>Institute for Alpine Environment, Eurac Research, Viale Druso 1, 39100 Bozen-Bolzano,  
11 Italy

12 <sup>4</sup>CISMA S.r.l., Via Volta 13/A, 39100 Bozen-Bolzano, Italy

13 <sup>5</sup>Eco-Research S.r.l., Via Negrelli 13, 39100 Bozen-Bolzano, Italy

14

15 *Correspondence to:* Michael Engel (Michael.Engel@unibz.it)

16

17 **Abstract**

18 The understanding of the hydrological and hydrochemical functioning of glacierized  
19 catchment requires the knowledge of the different controlling factors and their mutual  
20 interplay. For this purpose, the present study was carried out in two sub-catchments of the  
21 Sulden River catchment (130 km<sup>2</sup>, Eastern Italian Alps) in 2014 and 2015, characterized by  
22 similar size but contrasting geological setting. Samples were taken at different space and time  
23 scales for analysis of stable isotopes of water, electrical conductivity, major, minor and trace  
24 elements.

25 At the monthly sampling scale for different spatial scales (0.05 – 130 km<sup>2</sup>), complex spatial  
26 and temporal dynamics such as contrasting EC gradients in both sub-catchments were found.  
27 At the daily scale, for the entire Sulden catchment the relationship between discharge and  
28 electrical conductivity showed a monthly hysteretic pattern. Hydrometric and geochemical  
29 dynamics were controlled by an interplay of meteorological conditions and geological  
30 heterogeneity. After conducting a PCA analysis, the largest share of variance (36.3 %) was



31 explained by heavy metal concentrations (such as Al, V, Cr, Ni, Zn, Cd, Pb) during the  
32 melting period while the remaining variance (16.3 %) resulted from the bedrock type in the  
33 upper Sulden sub-catchment (inferred from EC, Ca, K, As and Sr concentrations). Thus, high  
34 concentrations of As and Sr in rock glacier outflow may more likely result from bedrock  
35 weathering. Furthermore, nivo-meteorological indicators such as maximum daily global solar  
36 radiation, three day maximum air temperature, and 15 day snow depth differences could  
37 explain the monthly conductivity and isotopic dynamics best. The decrease of snow depth  
38 calculated for different time lengths prior to the sampling day showed best agreements with  
39 conductivity and isotopic dynamics when time lengths varied. These insights may help to  
40 better predict hydrochemical catchment responses linked to meteorological and geological  
41 controls and to guide future classifications of glacierized catchments according to their  
42 hydrochemical characteristics.

43

## 44 **1 Introduction**

45 Runoff from glacierized catchments is an important fresh water resource to downstream areas  
46 (Kaser et al., 2010; Viviroli et al., 2011). High-elevation environments face rapid and  
47 extensive changes through retreating glaciers, reduced snow cover, and permafrost thawing  
48 (Harris et al., 2001; Dye, 2002; Beniston, 2003; Galos et al., 2015). This will have impacts on  
49 runoff seasonality, water quantity and water quality (Beniston 2006; Ragettli et al., 2016;  
50 Gruber et al., 2017). It is therefore of uttermost importance to better understand the behaviour  
51 of high-elevation catchments and their hydrological and hydrochemical responses at different  
52 spatial and temporal scales in view of water management, water quality, hydropower, and  
53 ecosystem services under the current phase of climate change (Beniston, 2003; Viviroli et al.,  
54 2011; Beniston and Stoffel, 2014).

55 In general, the hydrological response of catchments (i.e. runoff dynamics) are controlled by  
56 heterogeneous catchment properties (Kirchner, 2009), which become more diverse in  
57 catchments with large complexity of various landscape features, as it is the case of  
58 mountainous, high-elevation glacierized catchments (Cook and Swift, 2012). In fact, those  
59 catchments are deemed as highly dynamic geomorphological, hydrological and  
60 biogeochemical environments (Rutter et al., 2011). Understanding the interactions of controls  
61 driving the catchment response represents the key focus of studies in catchment hydrology



62 (Troch et al., 2015). The advances of tracer and isotope hydrology made during the last  
63 decades can substantially contribute to this objective, in order to gain more insights into the  
64 variability of different runoff components (Vaughn and Fountain, 2005; Maurya et al., 2011;  
65 Xing et al., 2015), catchment conceptualization (Baraer et al., 2015; Penna et al., 2017), and  
66 sensitivity to climate change (Kong and Pang, 2012).

67 In general, the main controls of hydrological and hydrochemical catchment responses are  
68 represented by climate, bedrock geology, surficial geology, soil, vegetation, and topography  
69 with drainage network (Devito et al., 2005; Carrillo et al., 2011; Williams et al 2015) and  
70 catchment shape (Sivapalan 2003). First, a major role is attributed to the global and regional  
71 climate, having strong impacts on mountain glaciers and permafrost, streamflow, water  
72 quality, water temperature, and suspended sediment yield (Milner et al., 2009; Moore et al.,  
73 2009; IPCC, 2013). The impact of climate is difficult to assess because it requires long time  
74 windows (e.g., decades), whereas meteorological drivers interact at a smaller temporal scales  
75 and thus are easier to address. Among different meteorological drivers, radiation fluxes at the  
76 daily time scale were identified as main energy source driving melting processes in  
77 glacierized catchments in different climates (Sicart et al., 2008). Beside radiation, air  
78 temperature variations correlate well with runoff under the presence of snow cover (Swift et  
79 al., 2005) and may affect streamflow seasonality when specific thresholds are exceeded  
80 (Cortés et al., 2011).

81 With respect to geology, it sets the initial conditions for catchment properties and drives its  
82 evolution (Carrillo et al., 2011). The geological setting strongly controls catchment  
83 connectivity, drainage, and groundwater discharge (Farvolden 1963), runoff response (Onda  
84 et al., 2001), residence time (Katsuyama et al., 2010), hydrochemistry during baseflow  
85 conditions (Soulsby et al., 2006a) and melting periods (Hindshaw et al., 2011), and subglacial  
86 weathering (Brown and Fuge, 1998). Also geomorphological features such as talus fields may  
87 affect streamflow and water quality, resulting from different flow sources and flow pathways  
88 (Liu et al., 2004). Catchment storage, as determined by both geology and topography, was  
89 found to impact the stream hydrochemistry as well (Rinaldo et al., 2015).

90 The hydrological conditions of the catchment are also a relevant driver of hydrological  
91 response and commonly refer to the antecedent soil moisture conditions to describe the state  
92 of the catchment and represent the hydrological connectivity (Uhlenbrook and Hoeg, 2003;  
93 Freyberg et al., 2017). Specifically in high elevation and high latitude catchments, also



94 permafrost thawing affects the hydrological connectivity (Rogger et al., 2017), leading to a  
95 strong control on catchment functioning as it drives the partitioning, storage and release of  
96 water (Tetzlaff et al., 2014). In more detail, retreating permafrost may also result in distinct  
97 geochemical signatures (Clark et al., 2001) and the release of heavy metals being previously  
98 stored in the ice (Thies et al., 2007; Krainer et al., 2015). This does not affect only the water  
99 quality but also the aquatic biota such as macroinvertebrate communities in these  
100 environments (Milner et al., 2009). Different weathering processes between the subglacial and  
101 periglacial environment can be found, resulting in a shift in chemical species and  
102 concentrations in the water (Anderson et al., 1997).

103 However, only few studies have investigated the geological, meteorological, and topographic  
104 controls on catchment response and stream water hydrochemistry in glacierized or  
105 permafrost-dominated catchments (Wolfe and English, 1995; Hodgkins, 2001; Lewis et al.,  
106 2012).

107 In this paper, we aim to fill this gap presenting data from a two year monitoring campaign  
108 where samples for stable isotopes of water, electrical conductivity (EC), major, minor and  
109 trace elements analysis were collected for two nearby glacierized catchments in the Eastern  
110 Italian Alps, characterized by similar size and climate and but contrasting geological setting.

111 The present study builds up on the following hypotheses: (1) bedrock-specific geochemical  
112 signatures reveal the geographic origin of water sources, (2) dilution effects and isotopic  
113 depletion in stream hydrochemistry are explained better by nivo-meteorological indicators  
114 controlling melt processes by radiation and air temperature than by precipitation-related  
115 indicators and (3) catchment controls not varying in short periods (such as geology and  
116 topography) lead to spatial variation in hydrochemistry while short-term controls (such as  
117 meteorological conditions) affect the temporal variations of hydrochemistry.

118 Specifically, we aim to:

- 119 • assess the spatio-temporal variability of the hydrochemical signature of stream water  
120 during melting and baseflow conditions;
- 121 • identify the hydrochemical signature of thawing permafrost and its role on stream  
122 water;



- 123       • analyse the capability of nivo-meteorological indicators to describe the  
124           hydrochemical signature of stream water.

## 125    **2 Study area and instrumentation**

### 126    **2.1 The Sulden river catchment**

127    The study was carried out in the Sulden/Solda River catchment, located in the upper  
128    Vinschgau/Venosta Valley (Eastern Italian Alps) (Fig. 1). The size of the study area is about  
129    130 km<sup>2</sup> defined by the stream gauge station of the Sulden River at Stilfserbrücke/ Ponte  
130    Stelvio (1110 m a.s.l.). The highest elevation is represented by the Ortler/ Ortlers peak (3905  
131    a.s.l.) within the Ortles-Cevedale group. A major tributary is the Trafoi River, joining the  
132    Sulden River close to the village Trafoi-Gomagoi. At this location, two sub-catchments,  
133    namely Sulden and Trafoi sub-catchment (75 and 51 km<sup>2</sup>, respectively) meet.

134    The study area has a current glacier extent of about 17.7 km<sup>2</sup> (14 % of the study area) and is  
135    slightly higher in the Trafoi than in the Sulden sub-catchment (17 % and 12 %, respectively).  
136    Main glacier tongues in the study area are represented by the Madatsch glacier (Trafoi sub-  
137    catchment) and Sulden glacier (Sulden sub-catchment). Geologically, the study area belongs  
138    to the Ortler-Campo-Cristalin (Mair et al., 2007). While permotriassic sedimentary rocks  
139    dominate the Trafoi sub-catchment, Quarzphyllite, Orthogneis, and Amphibolit are present in  
140    the Sulden sub-catchment. However, both catchments share the presence of orthogneis,  
141    paragneis and mica schist from the lower reaches to the outlet. Permafrost is sparsely located  
142    between 2400 and 2600 m a.s.l. and more frequent above 2600 m a.s.l. (Boeckli et al., 2012).  
143    Climatically, the mean annual air temperature is about -1.6 °C and the mean annual  
144    precipitation is about 1008 mm (2009 - 2016) at 2825 m a.s.l. (Hydrographic Office,  
145    Autonomous Province of Bozen-Bolzano). Due to the location of the study area in the inner  
146    dry Alpine zone, these precipitation amounts are relatively low compared to the amounts at  
147    similar elevation in the Alps (Schwarb, 2000). Further climatic data regarding the sampling  
148    period of this study are shown in Table 1. The study area lies within the National Park “Stelvio  
149    / Stilfser Joch” but it also includes ski slopes and infrastructures, as well as hydropower weirs.



150 **2.2 Meteorological, hydrometric and topographical data**

151 Precipitation, air temperature, humidity and snow depth is measured by an ultrasonic sensor at  
152 10 min measuring interval at the automatic weather station (AWS) Madritsch/Madriccio at  
153 2825 m a.s.l. (run by the Hydrographic Office, Autonomous Province of Bozen-Bolzano). We  
154 take data from this station as representative for the glacier in the catchment at similar  
155 elevation. At the outlet at Stilsferbrücke/Ponte Stelvio, water stages are continuously  
156 measured by an ultrasonic sensor (Hach Lange GmbH, Germany) at 10 min measuring  
157 interval and converted to discharge via salt dilution/photometric measurements (measurement  
158 range: 1.2 – 23.2 m<sup>3</sup> s<sup>-1</sup>; n=22). Turbidity is measured by a SC200 turbidity sensor (Hach  
159 Lange GmbH, Germany) at 5 min measuring interval. EC is measured by a TetraCon 700 IQ  
160 (WTW GmbH, Germany) at 1 second measuring interval. Both datasets were resampled to 10  
161 min time steps. All data used in this study are recorded and presented in solar time.  
162 Topographical data (such as catchment area and 50 m elevation bands) were derived from a  
163 2.5 m DEM using GIS processing (ArcGIS 10, ESRI).

164 **2.3 Tracer sampling and analysis**

165 Continuous stream water sampling at the outlet was performed by an automatic sampling  
166 approach using an ISCO 6712 system (Teledyne Technologies, USA). Generally, daily water  
167 sampling took place from mid-May to mid-October 2014 and 2015 (on 331 days) at 23:00 to  
168 ensure consistent water sampling close to the discharge peak and respecting its seasonal  
169 variation. In addition, grab samples from different stream locations, tributaries, and springs in  
170 the Sulden and Trafoi sub-catchments and the outlet were taken monthly from February 2014  
171 to November 2015 (Table 2). Samples were collected approximately at the same time (within  
172 less of an hour of difference) on all occasions. In winter, however, a different sampling time  
173 had to be chosen for logistical constraints (up to four hours of difference between both  
174 sampling times). However, this did not produce a bias on the results due to the very limited  
175 variability of the hydrochemical signature of water sources during winter baseflow conditions.  
176 Two active rock glaciers, located on Quarzphyllite bedrock in the upper Sulden sub-  
177 catchment, were selected to represent meltwater from permafrost. At the base of the steep  
178 rock glacier front, three springs at about 2600 m a.s.l. were sampled monthly from July to  
179 September 2014 and July to October 2015. Snowmelt water was collected as dripping water



180 from snow patches from April to September 2014 and March to October 2015 (n = 48  
181 samples), mainly located on the west to north-facing slopes of the Sulden sub-catchment and  
182 at the head of the valley in the Trafoi sub-catchment. Glacier melt water was taken only at the  
183 eastern tongue of the Sulden glacier from July to October 2014 and 2015 (n = 11 samples) for  
184 its safe accessibility. Precipitation samples were derived from bulk precipitation collectors,  
185 built according to the standards of the International Atomic Energy Agency (International  
186 Atomic Energy Agency 2014). They were placed at four different locations covering an  
187 elevations gradient of 1750 m and emptied on a monthly basis from April to November 2014  
188 and 2015. Only the precipitation collector at the mountain hut Schaubach remained during  
189 winter 2014/2015 to collect winter precipitation. Due to limited accessibility mainly in spring  
190 and autumn, the collector was emptied after more than one month. Snow samples were  
191 derived from snow profiles as integrated and layer-specific samples, which were dug along an  
192 elevation gradient once a month from January to April 2015 and after snowfall events in  
193 August to October 2015.

194 EC was measured in the field by a portable conductivity meter WTW 3410 (WTW GmbH,  
195 Germany) with a precision of  $\pm 0.1 \mu\text{S cm}^{-1}$  (nonlinearly corrected by temperature  
196 compensation at 25 °C).

197 All samples were stored in 50 ml PVC bottles with a double cap and no headspace. The  
198 samples were kept in the dark at 4°C in the fridge before the analysis.  $\delta^2\text{H}$  and  $\delta^{18}\text{O}$  isotopic  
199 composition of all water samples (except the ISCO stream water samples at the outlet) were  
200 analysed at the Laboratory of Isotope and Forest Hydrology of the University of Padova  
201 (Italy), Department of Land, Environments, Agriculture and Forestry by an off-axis integrated  
202 cavity output spectroscope (model DLT-100 908-0008, Los Gatos Research Inc., USA). The  
203 analysis protocol and the description of reducing the carry-over effect are reported in (Penna  
204 et al., 2010, 2012). The instrumental precision (as an average standard deviation of 2094  
205 samples) is 0.5‰ for  $\delta^2\text{H}$  and 0.08‰ for  $\delta^{18}\text{O}$ .

206 The  $\delta^{18}\text{O}$  isotopic composition of the ISCO stream water samples was analysed by an isotopic  
207 ratio mass spectrometer (GasBenchDelta V, Thermo Fisher) at the Free University of Bozen-  
208 Bolzano. Following the gas equilibration method (Epstein and Mayeda, 1953), 200- $\mu\text{l}$  sub-  
209 samples were equilibrated with He-CO<sub>2</sub> gas at 23 °C for 18 h and then injected into the  
210 analyser. The isotopic composition of each sample was calculated from two repetitions, and  
211 the standard deviation was computed. The instrumental precision for  $\delta^{18}\text{O}$  was  $\pm 0.2\%$ . We



212 applied a correction factor, described in Engel et al. (2016), to adjust the isotopic  
213 compositions of  $\delta^{18}\text{O}$  measured by the mass spectrometer to the ones measured by the laser  
214 spectroscope.

215 The analysis of major, minor and trace elements (Li, B, Na, Mg, Al, K, Ca, V, Cr, Mn, Fe,  
216 Co, Ni, Cu, Zn, Rb, Sr, Mo, Ba, Pb and U) was carried out by Inductively Coupled Plasma  
217 Mass Spectroscopy (ICP-MS ICAP-Q, Thermo Fischer) at the laboratory of EcoResearch srl.  
218 (Bozen-Bolzano).

#### 219 **2.4 Data analysis**

220 In order to better understand the effect of meteorological controls at different time scales, in  
221 particular precipitation and melting rates, different environmental variables derived from  
222 precipitation, air temperature, solar radiation and snow depth data from AWS Madritsch, were  
223 calculated (Table 3). Then, a sensitivity analysis was performed, which was based on a 1 day  
224 incremental time step and a temporal length of 30 days to respect the period of time between  
225 the monthly stream water samplings. As precipitation indicators, we considered the cumulated  
226 precipitation  $P$  in a period between 1 and 30 days prior to the sampling day, and the period of  
227 time  $D_{\text{prec}}$  in days starting from 1, 10 or 20 mm of cumulated precipitation occurred prior to  
228 the sampling day. As snow and ice melt indicators, we selected the maximum air temperature  
229  $T_{\text{max}}$  and maximum global solar radiation  $G_{\text{max}}$  in a period between 1 and 30 days prior the  
230 sampling day. Moreover, we calculated the difference of snow depth  $\Delta\text{SD}$  measured at the  
231 sampling day and the previous days, varying from 1 to 30 days. The temporal sensitivities of  
232 agreement between nivo-meteorological indicators and tracer signatures were expressed as  
233 Pearson correlation coefficients ( $p < 0.5$ ) and represented a measure to obtain the most  
234 relevant nivo-meteorological indicators.

235 In order to understand the link among water sources and their hydrochemical composition, a  
236 principle component analysis (PCA), using data centred to null and scaled to variance one (R  
237 core team, 2016), was performed. Data below detection limit were excluded from the  
238 analysis.

239 To assess the dampening effect of meltwater on stream water chemistry during baseflow  
240 conditions and the melting period, the variability coefficient (VC) was calculated following  
241 Eq. (1):

$$242 \text{ Variability coefficient } VC = \frac{SD_{\text{baseflow}}}{SD_{\text{melting}}} \quad (1)$$





243  $SD_{\text{baseflow}}$  is the standard deviation of stream EC sampled during baseflow conditions in winter  
244 at a given location and  $SD_{\text{melting}}$  is the one at the same locations during the melt period in  
245 summer (following Sprenger et al., 2016).

246 A two-component hydrograph separation (HS) based on EC and  $\delta^2\text{H}$  was assigned to separate  
247 the runoff contributions originating from the Sulden and Trafoi sub-catchment at each  
248 sampling moment during monthly sampling (Sklash and Farvolden, 1979), following Eq. (2)  
249 and Eq. (3):

$$250 \quad Q_{S1} = Q_{S2} + Q_{T1} \quad (2)$$

$$251 \quad P_{T1} = (C_{S2} - C_{S1}) / (C_{S2} - C_{T1}) \quad (3)$$

252 where P is the runoff proportion, C is the electrical conductivity EC or isotopic composition  
253 in  $^2\text{H}$  measured at the locations S1 (outlet), S2 (sampling location in the Sulden sub-  
254 catchment upstream the confluence with Trafoi River), and T1 (sampling location in the  
255 Trafoi sub-catchment upstream the confluence with Sulden River). While T1 served as "old  
256 water" component, S2 represented the "new water" component at S1. The uncertainty in the  
257 two-component HS was expressed as Gaussian error propagation using the instrumental  
258 precision of the conductivity meter ( $0.1 \mu\text{S cm}^{-1}$ ) and sample standard deviation from the laser  
259 spectroscope, following Genereux (1998). Furthermore, statistical analysis were performed to  
260 test the variance of hydrochemical data by means of a t-test (if data followed normal  
261 distribution), otherwise the nonparametric Mann-Whitney test was used.

## 262 **3 Results**

### 263 **3.1 Origin of water sources**

264 The isotopic signature of all water samples collected in the study area is shown in Fig. 2.  
265 Based on the isotopic signature of precipitation samples, the Local Meteoric Water Line  
266 (LMWL) was close to the Global Meteoric Water Line (GMWL). The isotopic signature of  
267 the other water sources fell on the water line, indicating that they originated from the same  
268 water vapour source as precipitation, with no or negligible secondary post-depositional  
269 fractionation. In more detail, rainfall samples represented the most enriched water source in  
270 the catchment ( $\delta^2\text{H}$ : -128.6 to -15.14 ‰) while snow was the most depleted one ( $\delta^2\text{H}$ : -196.3  
271 to -86.7 ‰) and became more enriched through melting processes, with a smaller isotopic  
272 variability ( $\delta^2\text{H}$ : -137.33 to -88.0 ‰). In contrast, glacier melt and rock glacier spring water



273 were isotopically relatively similar and slightly more positive than snowmelt ( $\delta^2\text{H}$ : -105.7 to -  
274 82.2 ‰, and -113.9 to -90.6 ‰, respectively). The isotopic range of spring water from the  
275 valley bottom (TSPR1-2, SSPR1) was relatively similar to the one of snowmelt ( $\delta^2\text{H}$ : -105.7  
276 to -88.8 ‰), with slightly more enriched samples from the Trafoi sub-catchment than from  
277 the Sulden sub-catchment. Only few water samples (i.e. snowmelt samples) plotted below the  
278 LMWL likely as a result of kinetic, non-equilibrium isotopic fractionation during the  
279 snowpack melting process (inset of Fig. 2).

280 To identify the geographic origin of stream water within the catchment, element  
281 concentrations of stream and rock glacier spring water are presented in Table 4 and 5. It is  
282 worth highlighting that heavy metal concentrations (such as Al, V, Cr, Ni, Zn, Cd, Pb)  
283 showed highest concentrations during intense melting in July 2015 at all six locations (partly  
284 exceeding concentration thresholds for drinking water (see European Union (Drinking Water)  
285 Regulations 2014). Element concentrations were clearly higher at the most upstream sampling  
286 locations. Relatively low variability coefficients ( $\text{VC} < 0.3$ ) for these elements confirmed that  
287 larger variations of concentrations occurred during the melting period and not during  
288 baseflow conditions. Interestingly, the highest heavy metal concentrations (such as Mn, Fe,  
289 Cu, Pb) of rock glaciers springs SPR2 – 4 delayed the heavy metal concentration peak in the  
290 stream by about two months.

291 In contrast, other element concentrations (such as As, Sr, K, Sb) generally revealed higher  
292 concentrations during baseflow conditions and lower concentrations during the melting  
293 period. This observation was corroborated by relatively high variability coefficients for As  
294 ( $\text{VC}$ : 2 – 2.9) and Sb ( $\text{VC}$ : 2 – 2.2) at S1, S2, and T1. For example, while highest Sr  
295 concentrations were measured at S6, As was highest at the downstream locations T1, S2, and  
296 S1. Regarding the rock glacier springs, their hydrochemistry showed a gradual decrease in As  
297 and Sr concentration from July to September 2015. The observed geochemical patterns are  
298 confirmed by PCA results (Fig. 3) and the correlation matrix (Fig. 4), revealing that  
299 geochemical dynamics are driven by temporal (PC1) and spatial controls (PC2) and a typical  
300 clustering of elements, respectively. PC1 shows high loadings for heavy metal concentrations  
301 (such as Al, V, Cr, Ni, Zn, Cd, Pb), supporting the clear temporal dependency for the entire  
302 catchment (baseflow conditions vs. melting period)(Fig. 3a). PC2 is instead mostly  
303 characterized by high loadings of  $\delta^2\text{H}$  and  $\delta^{18}\text{O}$  in the Trafoi sub-catchment (i.e. T1 and TT2)  
304 and geochemical characteristics (EC, Ca, K, As and Sr) from the upstream region of the



305 Sulden River and rock glacier spring water (i.e. S6 and SSPR2-4, respectively). Overall,  
306 temporal and spatial controls explained a variance of about 53 %.

### 307 **3.2 Temporal and spatial tracer variability**

308 The temporal and spatial variability of EC in the Sulden and Trafoi River along the different  
309 sections, their tributaries, and springs is illustrated in Fig. 5. Results highlight the dominant  
310 impact of water enriched in solutes during baseflow conditions starting from late autumn to  
311 early spring prior to the onset of the melting period. Such an impact seemed to be highest in  
312 water from streams and tributaries reaching the most increased conductivity at S6, ranging  
313 from 967 to 992  $\mu\text{S cm}^{-1}$  in January to March 2015. During the same period of time, isotopic  
314 composition was slightly more enriched and spatially more homogeneous among the stream,  
315 tributaries, and springs than in the summer months. In contrast, during the melting period,  
316 water from all sites in both sub-catchments became diluted due to different inputs of  
317 meltwater (Fig. 5 a, b), while water was most depleted during snowmelt dominated periods  
318 and less depleted during glacier melt dominated periods (Fig. 5c and 5d). Rainfall became a  
319 dominant runoff component during intense storm events. For instance, on 24 September 2015,  
320 a storm of 35 mm  $\text{d}^{-1}$  resulted in the strongest isotopic enrichment of this study, which is  
321 visible in Fig. 5c at T3 and TT2 ( $\delta^2\text{H}$  -86.9 ‰;  $\delta^{18}\text{O}$ : -12.4 ‰).

322 Hereinafter, the hydrochemistry of the Sulden and Trafoi sub-catchment is analyzed in terms  
323 of hydrochemical patterns of the main stream, tributaries, springs, and runoff contributions at  
324 the most downstream sampling location above the confluence. At T1 and S2, hydrochemistry  
325 was statistically different in its isotopic composition (Mann-Whitney Rank Sum Test:  $p <$   
326 0.001) but not in EC (Mann-Whitney Rank Sum Test:  $p = 0.835$ ). Runoff originating from  
327 Trafoi and derived from the two-component HS, contributed to the outlet by about 36 %  
328 ( $\pm 0.004$ ) to 58 % ( $\pm 0.003$ ) when using EC and ranged from 29 % ( $\pm 0.09$ ) to 83 % ( $\pm 0.15$ )  
329 when using  $\delta^2\text{H}$ . Thus, runoff at the outlet was sustained more strongly by the Trafoi River  
330 during non-melting periods while the runoff from the Sulden sub-catchment dominated during  
331 the melting period.

332 By the aid of both tracers, catchment specific hydrochemical characteristics such as  
333 contrasting EC gradients along the stream were revealed (Fig. 5 and Fig. 6). EC in the Trafoi



334 River showed linearly increasing EC with increasing catchment area (from T3 to T1) during  
335 baseflow and melting periods ('EC enrichment gradient').

336 In contrast, the Sulden River revealed relatively high EC at the highest upstream location (S6)  
337 and relatively low EC upstream the confluence with the Trafoi River (S2) during baseflow  
338 conditions. The exponential decrease in EC ('EC dilution gradient') during this period of time  
339 was strongly linked to the catchment area. Surprisingly, the EC dilution along the Sulden  
340 River was still persistent during melting periods but highly reduced. In this context, it is also  
341 interesting to compare the EC variability (expressed as VC) along Trafoi and Sulden River  
342 during baseflow conditions and melting periods (Table 6). For both streams, VC increased  
343 with decreasing distance to the confluence (Trafoi River) and the outlet (Sulden River), and  
344 thus representing an increase in catchment size. The highest EC variability among all stream  
345 sampling locations is given by the lowest VC, which was calculated for S6. This location  
346 represents the closest one to the glacier terminus and showed a pronounced contrast of EC  
347 during baseflow conditions and melting periods (see Fig. 5 and Fig. 6).

348 Regarding the hydrochemical characterisation of the tributaries in both sub-catchments (Fig.  
349 5), Sulden tributaries were characterised by a relatively low EC variability (68.2 – 192.3  $\mu\text{S}$   
350  $\text{cm}^{-1}$ ) and more negative isotopic values ( $\delta^2\text{H}$ : -100.8 – 114.5 ‰) compared to the higher  
351 variability in hydrochemistry of the Sulden River. In contrast, the tracer patterns of Trafoi  
352 tributaries were generally consistent with the ones from the stream. Generally, also spring  
353 water at TSPR1, TSPR2, and SSPR1 followed these patterns during baseflow and melting  
354 periods in a less pronounced way, possibly highlighting the impact of infiltrating snowmelt  
355 into the ground. Comparing both springs sampled in the Trafoi sub-catchment indicated that  
356 spring waters were statistically different only when using EC (Mann-Whitney Rank Sum  
357 Test:  $p = 0.039$ ). While TSPR1 hydrochemistry was slightly more constant, the one of TSPR2  
358 was more variable from June to August 2015 (Fig. 5). This may result from different flow  
359 paths and disconnected recharge areas sustaining separately each spring, possibly pointing to  
360 a deeper (for TSPR1) and a shallower (for TSPR2) groundwater body.

### 361 **3.3 Temporal variability at the catchment outlet**

362 The temporal variability of the hydrochemical variables observed at the catchment outlet and  
363 of the meteorological drivers is illustrated in Fig. 7. Controlled by increasing radiation inputs  
364 and air temperatures above about 5°C in early summer (Fig. 7a and 7b), first snowmelt (as



365 indicated by a depleted isotopic signature of about -14.6 ‰ in  $\delta^{18}\text{O}$  and EC of about 200  $\mu\text{S}$   
366  $\text{cm}^{-1}$ ) induced runoff peaks in the Sulden River of about 20  $\text{m}^3 \text{s}^{-1}$  (starting from a winter  
367 baseflow of about 1.8  $\text{m}^3 \text{s}^{-1}$ ), as shown in Fig. 7c and 7e. Later in the summer, glacier melt  
368 induced runoff peaks reached about 13 – 18  $\text{m}^3 \text{s}^{-1}$ , which are characterised by relatively low  
369 EC (about 235  $\mu\text{S cm}^{-1}$ ) and isotopically more enriched stream water ( $\delta^{18}\text{O}$ : about -13.3 ‰).  
370 The highest discharge measured during the analysed period (81  $\text{m}^3 \text{s}^{-1}$  on 13 August 2014)  
371 was caused by a storm event, characterized by about 31 mm of precipitation falling over 3  
372 hours at AWS Madritsch. Unfortunately, isotopic data for this event were not available due to  
373 a technical problem with the automatic sampler.

374 Water turbidity was highly variable at the outlet, and mirrored the discharge fluctuations  
375 induced by meltwater or storm events. Winter low flows are characterised by very low  
376 turbidity (< 10 NTU, corresponding to less than 6  $\text{mg l}^{-1}$ ). In summer, turbidity ranged  
377 between 20 and up to 1200 NTU during cold spells and melt events combined with storms,  
378 respectively. However, the maximum value recorded was 1904 NTU reached after several  
379 storm events of different precipitation amounts (17 mm, 50 mm, and 9 mm) on 12, 13, and 14  
380 August 2014, respectively. Unfortunately, the turbidimeter did not work properly after the  
381 August 2014 flood peak, in mid-July 2015 and beginning of October 2015.

382 Furthermore, the interannual variability of meteorological conditions with respect to the  
383 occurrence of warm days, storm events and snow cover of the contrasting years 2014 and  
384 2015 is clearly visible and contributed to the hydrochemical dynamics (Fig.7 and Table 1).  
385 While about 250 cm of maximal snowpack depth in 2014 lasted until mid-July, only about  
386 100 cm were measured one year after with complete disappearance of snow one month  
387 earlier. In 2015, several periods of remarkable warm days occurred reaching more than 15°C  
388 at 2825 m a.s.l. and led to a catchment entirely under melting conditions (freezing level above  
389 5000 m a.s.l., assuming a lapse rate of 6.5  $\text{K km}^{-1}$ ). In contrast, warmer days in 2014 were less  
390 pronounced and frequent but accompanied by intense storms of up to 50  $\text{mm d}^{-1}$ . These  
391 meteorological conditions seem to contribute to the general hydrochemical patterns described  
392 above. Despite a relatively similar hydrograph with same discharge magnitudes during melt-  
393 induced runoff events in both years, EC and  $\delta^{18}\text{O}$  clearly characterized snowmelt and glacier  
394 melt-induced runoff events in 2014. However, a characteristic period of depleted or enriched  
395 isotopic signature was lacking in 2015 so that snowmelt and glacier melt-induced runoff  
396 events were graphically more difficult to distinguish.



397 The daily variations in air temperature, discharge, turbidity, and EC showed marked  
398 differences in the peak timing. Maximum daily air temperature generally occurred between  
399 12:00 and 15:00, resulting in discharge peaks at about 22:00 to 1:00 in early summer and at  
400 about 16:00 to 19:00 during late summer. Turbidity peaks were measured at 22:00 to 23:00 in  
401 May to June and clearly anticipated to 16:00 to 19:00 in July and August. In contrast, EC  
402 maximum occurred shortly after the discharge peak between 00:00 to 1:00 in early summer  
403 and at 11:00 to 15:00, clearly anticipating the discharge peaks.

404 It is interesting to highlight a complex hydrochemical dynamics during the baseflow period in  
405 November 2015, which was interrupted only by a rain-on-snow event on 28 and 29 October  
406 2015. This events was characterized by more liquid (12.9 mm) than solid precipitation (6.6  
407 mm) falling on a snowpack of about 10 cm (at 2825 m a.s.l.). While stream discharge showed  
408 a typical receding hydrograph confirmed by EC being close to the background value of about  
409  $350 \mu\text{S cm}^{-1}$ ,  $\delta^{18}\text{O}$  indicated a gradual isotopic depletion suggesting the occurrence of  
410 depleted water (e.g., snowmelt) in the stream. Indeed, also turbidity was more variable and  
411 slightly increased during this period.

412 To better characterize the temporal dynamics of hydrochemical variables, Fig. 8 shows the  
413 different relationships of discharge, EC,  $\delta^{18}\text{O}$ , and turbidity grouped for different months. In  
414 general, high turbidity seemed to be linearly correlated with discharge showing a monthly  
415 trend (Fig. 8a). In fact, this observation could be explained by generally higher discharges  
416 during melting periods (June, July, and August) and lower ones during baseflow conditions.  
417 Discharge and EC exhibited a relationship characterised by a hysteretic-like pattern at the  
418 monthly scale (Fig. 8b), which seemed to be associated with the monthly increasing  
419 contribution of meltwater with lower EC during melting periods contrasting with dominant  
420 groundwater contributions having higher EC during baseflow conditions.

421 During these periods,  $\delta^{18}\text{O}$  of stream water was mainly controlled by the dominant runoff  
422 components (i.e. snowmelt and glacier melt in early summer and mid- to late summer,  
423 respectively) rather than the amount of discharge (Fig. 8c). Similarly, the relationship  
424 between  $\delta^{18}\text{O}$  and EC was driven by the discharge variability resulting in a specific range of  
425 EC values for each month and by the meltwater component generally dominant during that  
426 period (Fig. 8d). As  $\delta^{18}\text{O}$  was dependent on the dominant runoff components and less on the  
427 amount of discharge, turbidity showed no clear relationship with the isotopic composition



428 (Fig. 8e). In contrast, EC and turbidity were controlled by monthly discharge variations so  
429 that both variables followed the monthly trend, revealing a linear relationship (Fig. 8f).

### 430 **3.4 Meteorological controls on hydrochemical stream responses within the catchment**

431 To identify the most significant correlations between stream hydrochemistry ( $\delta^2\text{H}$  and EC)  
432 and nivo-meteorological indicators (Table 3), the Pearson correlation coefficient was used.  
433 While significant correlations were generally found for maximum air temperature  $T_{\max}$  (only  
434 for EC), maximum global solar radiation  $G_{\max}$ , and the difference of snow depth  $\Delta\text{SD}$ , other  
435 indicators such as cumulated precipitation  $P_{\text{cum}}$  and  $D_{\text{Prec}}$  were not significant ( $p < 0.05$ ) and  
436 thus excluded from further analysis.

437 As the correlation of the most relevant nivo-meteorological indicators  $T_{\max}$ ,  $G_{\max}$ , and  $\Delta\text{SD}$   
438 may vary depending on specific lag times, results from the sensitivity analysis are shown in  
439 Fig. 9. In general,  $\Delta\text{SD}$  showed the highest positive correlations with tracers and were most  
440 sensitive for lag time of 1d, 5d, and 15d (Pearson correlation coefficient: 0.77, 0.63, and 0.85,  
441 respectively;  $p < 0.05$ ). Furthermore, regarding global solar radiation and maximum air  
442 temperature,  $G_{\max 1d}$  and  $T_{\max 3d}$  showed best agreements (Pearson correlation coefficient: -0.83  
443 and -0.7, respectively;  $p < 0.05$ ).

444 To explore possible relationships between stream hydrochemistry ( $\delta^2\text{H}$  and EC) and nivo-  
445 meteorological controls, selected indicators (at their most significant temporal scale)  $T_{\max 3d}$ ,  
446  $G_{\max 1d}$  and  $\Delta\text{SD}_{15d}$  are shown in Fig.10 and 11. Those indicators represented the main drivers  
447 of EC and  $\delta^2\text{H}$  variability within the Sulden and Trafoi catchment.

448 First, we observed that with increasing maximum air temperature  $T_{\max 3d}$ , EC concentration  
449 clearly decreased, strongly influenced by the dilution effect of meltwater. For example, an  
450 increase of  $T_{\max 3d}$  by 5°C (from 0° to 5°C) led to a decrease in EC in the Sulden and Trafoi  
451 River by about 15 – 154  $\mu\text{S cm}^{-1}$  while a change from 10° to 15°C resulted in a drop of EC of  
452 about 22 – 225  $\mu\text{S cm}^{-1}$  (Fig. 10a and b). Therefore, it can be noticed that the decrease in EC  
453 was highest with relatively high  $T_{\max 3d}$ . Interestingly, the dilution seemed to depend also on  
454 the sampling location along the stream and type of stream, as revealed by S6 (highest changes  
455 in EC) and ST2 (lowest changes in EC) locations in the Sulden sub-catchment.

456 Secondly, we analysed the relationship of EC concentration and global solar radiation. As  
457 shown in Fig. 10c to Fig. 10f, increasing maximum global solar radiation during the sampling



458 day  $G_{\max 1d}$  (from 1400 to 1600  $W m^{-2}$ ) in the Sulden and Trafoi River led to strongly  
459 decreased EC concentrations by about 94 – 382  $\mu S cm^{-1}$ . In agreement with  $T_{\max 3d}$ , the highest  
460 dilution effect was observed at S6. An isotopic depletion in  $\delta^2H$  of 2.9‰ was calculated for  
461 the Sulden River, while it notably was 7.1‰ for the Trafoi River.

462 Finally, we could explain the dilution effect also by the negative changes of snow depth  $\Delta SD$ ,  
463 which represented the most sensitive variable to the temporal length (1d, 5d, and 15d)  
464 compared to the other variables (Fig. 9). Using the example of  $\Delta SD_{15d}$  (measured at the  
465 sampling day and 15 days prior to the sampling day), EC concentrations in both sub-  
466 catchments resulted in less than 158 and 180  $\mu S cm^{-1}$  when losses of snow depths were about  
467 50 to 70 cm (Trafoi and S1 – S4 streams, respectively). Smaller losses from 10 to 20 cm were  
468 accompanied by still relatively high EC values of 256 and 301  $\mu S cm^{-1}$  (Trafoi and S1 – S4  
469 streams, respectively) but led to a drop in EC concentrations by about 35 to 42  $\mu S cm^{-1}$  in  
470 both sub-catchments. Therefore, the decrease in EC was highest with relatively high  $\Delta SD_{15d}$ .

471

472 With respect to  $\delta^2H$ , the dilution effect was associated with the typical isotopic depletion of  
473 stream water, confirming the stream water dilution due to snowmelt input. On the one hand,  
474 changes in snow depth from 60 to 50 cm of snow depth resulted in a depletion of 2.36 ‰ to  
475 2.79 ‰ and 2.24 to 2.59 ‰ in  $\delta^2H$  at Trafoi and Sulden (S1, S2, S5) streams, respectively. On  
476 the other hand, changes of snow depth of less than 20 cm led only to smaller isotopic  
477 depletion of 1.05 to 1.19 ‰ for the Trafoi and Sulden River. Not surprisingly, the clear linear  
478 relationship between  $\Delta SD$  and tracers held only for losses in snow depth. In contrast, positive  
479 changes in  $\Delta SD$  led to remarkably higher variability in EC and  $\delta^2H$  in the river network.

## 480 **4 Discussion**

### 481 **4.1 Comparison of meteoric water lines**

482 The geographic origin of water vapour can generally be inferred by comparing the LMWL to  
483 the GMWL (Craig 1961). Study results showed that precipitation was mainly formed by water  
484 vapour originated from the Atlantic Ocean, which was in general agreement with the findings  
485 of other studies. The LMWL of the Sulden catchment was very similar to the one from a  
486 station at 2731 m a.s.l. in the Vermigliana Valley ( $\delta^2H (\text{‰}) = 8 \delta^{18}O + 7.8$ ) (Chiogna et al.,  
487 2014) and a station at 2300 m a.s.l. in the Noce Bianco catchment ( $\delta^2H (\text{‰}) = 7.5 \delta^{18}O + 7.9$ ;





488  $R^2 = 0.97$ ,  $n=40$ ) (Carturan et al., 2016), located south between the Ortles-Cevedale and  
489 Adamello–Presanella group. However, it was slightly different in terms of d-excess when  
490 considering the LMWL of Matsch/Mazia Valley (d-excess: 10.3, Penna et al., 2014) and  
491 Northern Italy (d-excess: 9.4, Longinelli and Selmo, 2003). Moreover, it clearly differed from  
492 the Mediterranean Meteoric Water Line (MMWL:  $\delta^2\text{H} (\text{‰}) = 8 \delta^{18}\text{O} + 22$ ; Gat and Carmi,  
493 1970). These observations may confirm the presence of different precipitation patterns and  
494 microclimates at the regional scale (Brugnara et al., 2012).

#### 495 **4.2 Geological controls and hydrological connectivity**

496 Geochemical dynamics were driven by a pronounced release of heavy metals (such as Al, V,  
497 Cr, Ni, Zn, Cd, Pb) shown for the entire catchment and, in contrast, by a specific release of As  
498 and Sr in the upper and lower Sulden sub-catchment (Fig. 3). Yet, as the explained variance  
499 was only at about 53 %, further controls may be present. In this context, PC3 explained 11.8  
500 % of additional variance and may represent surface vs. subsurface flows or residence time  
501 within the soil.

502 With respect to the first observation, several sources of heavy metals can be addressed: on the  
503 one hand, these elements may be released by rock weathering on freshly-exposed mineral  
504 surfaces and sulphide oxidation, typically produced in metamorphic environments (Nordstrom  
505 et al., 2011). Proglacial stream hydrochemistry may also strongly depend on the seasonal  
506 evolution of the subglacial drainage system that contribute to specific element releases  
507 (Brown and Fuge, 1998). In this context, rock glacier thawing may play an important role for  
508 the release of Ni (Thies et al., 2007; Mair et al., 2011; Krainer et al., 2015) and Al and Mn  
509 (Thies et al., 2013). However, high Ni concentrations were not observed in this study.  
510 Moreover, high heavy metal concentrations were measured during the melting period in mid-  
511 summer, which would generally be too early to derive from permafrost thawing (Williams et  
512 al., 2006; Krainer et al., 2015). Also bedrock weathering as major origin probably needs to be  
513 excluded because low concentrations occurred in winter when the hydrological connectivity at  
514 higher elevations was still present (inferred from running stream water at the most upstream  
515 locations).

516 On the other hand, it is therefore more likely that heavy metals derive from meltwater itself  
517 due to the spatial and temporal dynamics observed. This would suggest that the element  
518 release is strongly coupled with melting and infiltration processes, when hydrological



519 connectivity within the catchment is expected to be highest. To support this explanation,  
520 supplementary element analysis of selected snowmelt ( $n = 2$ ) and glacier melt ( $n = 2$ ) samples  
521 of this study were conducted. Although these samples did not contain high concentrations of  
522 Cd, Ni, and Pb, for example, snowmelt in contact with the soil surface was more enriched in  
523 such elements than dripping snowmelt. Moreover, snowmelt and ice melt samples from the  
524 neighbouring Matsch/Mazia Valley in 2015 were strongly controlled by high Al, Co, Cd, Ni,  
525 Pb and Zn concentrations (Engel et al., 2017). As shown for 21 sites in the Eastern Italian  
526 Alps (Veneto and Trentino-South Tyrol region), hydrochemistry of the snowpack can largely  
527 be affected by heavy metals originating from atmospheric deposition from traffic and industry  
528 (such as V, Sb, Zn, Cd, Mo, and Pb) (Gabielli et al., 2006). Likely, orographically induced  
529 winds and turbulences arising in the Alpine valleys may often lead to transport and mixing of  
530 trace elements during winter. Studies from other regions, such as Western Siberia Lowland  
531 and the Tibetan Plateau, agree on the anthropogenic origin (Shevchenko et al., 2016 and Guo  
532 et al., 2017, respectively).

533 In contrast, with respect to the origin of As and Sr, a clear geological source can be attributed,  
534 supporting the first hypothesis on bedrock-specific geochemical signatures. In the lower  
535 Sulden catchment (i.e. S1, S2, and T1), As could mainly originate from As-containing  
536 bedrocks. As rich lenses are present in the cataclastic carbonatic rocks (realgar bearing) and in  
537 the mineralized, arsenopyrite bearing bands of quartzphyllites, micaschists and paragneisses  
538 of the crystalline basement. Different outcrops and several historical mining sites are known  
539 and described in the literature (Mair, 1996, Mair et al., 2002, 2009; Stingl and Mair, 2005). In  
540 the upper Sulden catchment, the presence of As is supported by the hydrochemistry of rock  
541 glacier outflows in the Zay sub-catchment (corresponding to the drainage area of ST2; Engel  
542 et al., 2018) but was not reported in other studies (Thies et al., 2007; Mair et al., 2011;  
543 Krainer et al., 2015; Thies et al., 2013). Also high-elevation spring waters in the Matsch  
544 Valley corroborated that As and Sr concentrations may originate from paragneisses and  
545 micaschists (Engel et al., 2017). In this context, we suggest a controlling mechanism as  
546 follows: the gradual decrease in As and Sr concentrations from rock glacier springs clearly  
547 disagrees with the observations from other studies that rock glacier thawing in late summer  
548 leads to increasing element releases (Williams et al., 2006; Thies et al., 2007; Krainer et al.,  
549 2015; Nickus et al., 2015). Therefore, it is more likely that As and Sr originate from the  
550 Quarzphyllite rocks, that form the bedrock of the rock glaciers (see Andreatta, 1952;



551 Montrasio et al., 2012). Weathering and former subglacial abrasion facilitate the release  
552 (Brown, 2002). As- and Sr-rich waters may form during winter when few quantities of water  
553 percolate in bedrock faults and then are released due to meltwater infiltration during summer  
554 (V. Mair, personal communication, 2018). As a clear delayed response of heavy metal  
555 concentrations in rock glacier outflow was revealed, the infiltration and outflow processes  
556 along flow paths in the bedrock near the rock glaciers may take up to two months to  
557 hydrochemically respond to snowmelt contamination.

558 As a consequence, a clear hydrochemical signature of permafrost thawing is difficult to find  
559 and results may lack the transferability to other catchments as not all rock glaciers contain  
560 specific elements to trace (Colombo et al., 2017). In this context, as precipitation and  
561 snowmelt affect the water budget of rock glaciers (Krainer and Mostler, 2002; Krainer et al.,  
562 2007), potential impacts of atmospheric inputs on rock glacier hydrochemistry could be  
563 assumed and would deserve more attention in future (Colombo et al., 2017).

564 Furthermore, export of elements in fluvial systems is complex and may strongly be affected  
565 by the pH (Nickus et al., 2015) or interaction with solids in suspension (Brown et al., 1996),  
566 which could not be addressed in this study. Further insights on catchment processes might be  
567 gained considering also element analysis of the solid fraction, to investigate whether water  
568 and suspended sediment share the same provenance.

### 569 **4.3 The role of nivo-meteorological conditions and topography**

570 Superimposing the impact of the geological origin, melting processes were controlled by  
571 meteorological conditions and topography, affecting stream hydrochemistry during summer,  
572 as shown by isotope dynamics (Fig. 5 and 7) and hydrochemical relationships (Fig. 8). It is  
573 well known that high correlations between snow or glacier melt and maximum air  
574 temperature exist (U.S. Army Corps of Engineers 1956; Braithwaite 1981), thus controlling  
575 daily meltwater contributions to streamflow (Mutzner et al., 2015; Engel et al., 2016). While  
576  $\Delta S D$  was used in this study, also snow depth and the extent of snow cover are suggested as  
577 effective indicators, exhibiting a strong control on runoff dynamics and thus melting  
578 processes (Singh et al., 2005). Likely, more specific explanatory variables such as vapour  
579 pressure, net radiation, and wind (Zuzel and Cox, 1975) or turbulent heat fluxes and long-  
580 wave radiation (Sicart et al., 2006) may exist but were not included in the present study due to  
581 the lack of observations.



582 As shown in this study, dilutions effects and isotopic depletion could rather be explained by  
583 maximum values  $T_{\max 3d}$  and  $G_{\max 1d}$  than averages of nivo-meteorological indicators or  
584 precipitation-related indicators. This result confirms the second hypothesis on the importance  
585 of nivo-meteorological indicators controlling melt processes by radiation and air temperature.  
586 Such observation may imply the importance of threshold-like controls at the daily and short-  
587 term scale, leading to tipping points along the cascade from atmospheric circulation and local  
588 climate to hydrology to physico-chemical habitat (Milner et al., 2009). In this regard, the  
589 (cumulated) daily maximum positive air temperature was used to characterize the decay of  
590 simulated snow albedo related to snow metamorphism (Ragetti and Pellicciotti, 2012). The  
591 authors also defined a threshold temperature for melt onset of 5°C, being in agreement with  
592 our findings (shown in Fig. 7, Fig. 10a, and Fig. 10b). Moreover, relatively small changes and  
593 low indicator values led to hydrochemical changes in stream water composition. This could  
594 be justified by the fact that nivo-meteorological indicators were derived from 2825 m a.s.l.,  
595 meaning that only about 30 % of the catchment area (assuming elevation bands of 50 m) were  
596 above this location. Therefore, meteorological conditions and related nivo-meteorological  
597 indicator may be more sensitive when compared to hydrochemical responses of the entire  
598 catchment. While favourable melting conditions are certainly delayed at higher elevations,  
599 stream water composition detected along the Sulden and Trafoi River (except S6 being closest  
600 to the weather station) would mainly reflect melting processes originating from the lower  
601 reaches within the catchment.

602 In this study, the most pronounced dilution effect and isotopic depletion (regarding monthly  
603 data) could be attributed to  $G_{\max 1d}$ , which thus may be considered as the most relevant nivo-  
604 meteorological indicator. This observation could be supported by Vincent and Six (2013),  
605 who found that spatial variations of ice ablation were mainly driven by potential solar  
606 radiation. It is further considered to be the main energy source driving melt processes in  
607 glacierized catchments of different climates (Sicart et al., 2008) and may integrate the effect  
608 of cloud coverage (Anslow et al., 2008). In contrast, lower radiation inputs and subzero air  
609 temperatures occurred during snowfall events (indicated by positive  $\Delta SD$ ) and likely  
610 interrupted melt processes, leading to higher variability of hydrochemical stream water  
611 composition (Hannah et al., 1999; Sicart et al., 2006; DeBeer and Pomeroy, 2010).

612 Results from the temporal sensitivity analysis are generally difficult to compare due to the  
613 lack of suitable studies and thus provide a novel data set for glacierized catchments. The



614 sensitivity of  $\Delta SD$  to different temporal length (3d, 5d, 15d) may indicate potential meltwater  
615 storage components and their effectiveness to route meltwater at different temporal scales.  
616 First, the snowpack represents a short-term storage for meltwater ranging from few hours to  
617 few days (Coléou and Lesaffre, 1998), due to different snowpack properties (i.e. irreducible  
618 water saturation, layer thickness) (Colbeck 1972; Marsh and Pomeroy, 1996). Second, the  
619 presence of slower and quicker flow paths within glacial till, talus, moraines, and shallow vs.  
620 deeper groundwater compartments could justify the intermediate (5d) and longer (15d)  
621 meltwater response (Brown et al., 2006; Roy and Hayashi, 2009; McClymont et al., 2010;  
622 Fischer et al., 2015; Weiler et al., 2017).

#### 623 **4.4 Implications for streamflow and hydrochemistry dynamics**

624 Tracer dynamics of EC and stable isotopes associated with monthly discharge variations  
625 generally followed the conceptual model of the seasonal evolution of streamflow  
626 contributions, as described for catchments with glacierized area of 17 % (Penna et al. 2017)  
627 and 30 % (Schmieder et al. 2017). However, isotopic dynamics were generally less  
628 pronounced compared to these studies, likely resulting from the impact of relative meltwater  
629 contribution related to different catchment sizes and the proportion of glacierized area (Baraer  
630 et al., 2015).

631 In addition, hydrometric and geochemical dynamics analysed in this study were controlled by  
632 an interplay of meteorological conditions and the heterogeneity of geology. Such an interplay  
633 is highlighted by EC dynamics (i.e. EC variability derived from VC), to be further controlled  
634 by the contributing catchment area (i.e. EC gradients along the Sulden and Trafoi River). As  
635 EC was highly correlated to Ca concentration (Spearman rank correlation: 0.6,  $p < 0.05$ ; see  
636 Fig. 4), EC dynamics were determined by the spatial distribution of different geology. For  
637 example, as dolomitic rocks are present almost within the entire Trafoi sub-catchment,  
638 meltwater following the hydraulic gradient can likely become more enriched in solutes with  
639 longer flow pathways and increasing storage capability related to the catchment size (Fig. 6).  
640 As consequence, the ‘EC enrichment gradient’ could persist during both the melting period  
641 and baseflow conditions in the presence of homogenous geology. Therefore, topography as  
642 control may become more important than the geological setting, to control spatial stream  
643 water variability. In the Sulden sub-catchment, however, dolomitic rocks are only present in  
644 the upper part of the catchment while metamorphic rocks mostly prevail. This leads to a



645 pronounced dilution of Ca-rich waters with increasing catchment area or in other words,  
646 increasing distance from the source area (Fig. 6) during baseflow conditions. This implies that  
647 meltwater contributions to the stream homogenize the effect of geographic origin on different  
648 water sources, having the highest impact in vicinity to the meltwater source (see Table 6).

649 The additional effect of topographical characteristics is underlined by the findings that the  
650 Sulden River hydrochemistry at S2 was significantly more depleted in  $\delta^2\text{H}$  and  $\delta^{18}\text{O}$  than T1  
651 hydrochemistry. Compared with the Sulden sub-catchment, the Trafoi sub-catchment has a  
652 slightly lower proportion of glacier extent but, more importantly, has a clearly smaller  
653 catchment area within the elevation bands of 1800 to 3200 m a.s.l. (i.e. 40.2 km<sup>2</sup> for the  
654 Trafoi and 66.5 km<sup>2</sup> for the Sulden sub-catchment). In this elevation range, the sub-  
655 catchments of major tributaries ST1, ST2, and ST3 are situated, which deliver large snowmelt  
656 contributions to the Sulden River (Fig. 6).

657 In consequence, resulting from the impact of these different controls, specific hydrometric  
658 and hydrochemical relationships derive. For example, the hysteretic relationship between  
659 discharge and EC (Fig. 8b) helps to identify the conditions with maximum discharge and EC:  
660 during baseflow conditions, the Sulden River showed highest EC of about 350  $\mu\text{S cm}^{-1}$   
661 seemingly to be bound to only about 3 m<sup>3</sup> s<sup>-1</sup> whereas the maximum dilution effect occurred  
662 during a storm on 29 June 2014 (55 mm of precipitation at AWS Madritsch) with 29.3 m<sup>3</sup> s<sup>-1</sup>  
663 of discharge resulting in only 209  $\mu\text{S cm}^{-1}$ . However, these observations based on daily data  
664 sampled at 23:00, likely not capturing the entire hydrochemical variability inherent of the  
665 Sulden catchment. As shown in Fig. 5 and Fig. 7, much higher discharges and thus even lower  
666 EC could be reached along the Sulden River and inversely, which was potentially limited by  
667 the specific geological setting of the study area.

668 As more extreme weather conditions (such as heat waves, less solid winter precipitation) are  
669 expected in future (Beniston, 2003; Viviroli et al., 2011; Beniston and Stoffel 2014),  
670 glacierized catchments may exhibit more pronounced hydrochemical responses such as  
671 shifted or broader ranges of hydrochemical relationships and increased heavy metal  
672 concentrations both during melting periods and baseflow conditions. However, identifying  
673 these relationships with changing meteorological conditions would deserve more attention  
674 and is strongly limited by our current understanding of underlying hydrological processes  
675 (Schaepli et al., 2007). In a changing cryosphere, more complex processes such as non-  
676 stationarity processes may emerge under changing climate, which itself was found to be a



677 major cause of non-stationarity (Milly et al., 2008). In this context, explaining the  
678 hydrochemical dynamics ambiguity observed during the baseflow period in November 2015  
679 (Fig. 7) will deserve further attention.

680 Finally, our results can partly confirm the third hypothesis following Heidebüchel et al. (2013).  
681 Long-term controls such as geology and topography govern hydrochemical responses at the  
682 spatial scale (such as bedrock-specific geochemical signatures, EC gradients, and relative  
683 snowmelt contribution). In contrast, short-term controls such as maximum daily solar  
684 radiation, air temperature, and snow depth differences drive short-term responses (such as  
685 discharge variability and EC dilution). However, as the catchment response strongly  
686 depended on the melting period vs. baseflow conditions, controls at longer temporal scales  
687 interact as well. Thus, our findings suggest that glacierized catchments react in a much more  
688 complex way and that catchment responses cannot be attributed to one specific scale, justified  
689 by either short-term or long-term controls alone.

690 In this context, the present study provides novel insights into geological, meteorological, and  
691 topographic controls of stream water hydrochemistry rarely addressed for glacierized  
692 catchments so far. Moreover, this study strongly capitalizes on an important dataset that  
693 combines nivo-meteorological indicators and different tracers (stable isotopes of water, EC,  
694 major, minor and trace elements), underlining the need for conducting multi-tracer studies in  
695 complex glacierized catchments.

#### 696 **4.5 Methodological limitation**

697 The sampling approach combined a monthly spatial sampling with daily sampling at the  
698 outlet, which methodologically is in good agreement with other sampling approaches,  
699 accounting for increasing distance of sampling points to the glacier (Zhou et al., 2014; Baraer  
700 et al., 2015), intense spatial and temporal sampling (Penna et al., 2014; Fischer et al., 2015),  
701 synoptic sampling (Carey et al., 2013; Gordon et al., 2015), and different catchment structures  
702 such as nested catchments (Soulsby et al., 2006b). Sampling covered a variety of days with  
703 typical snowmelt, glacier melt and baseflow conditions during 2014 and 2015, confirming the  
704 representativeness of tracer dynamics within two years contrasting in their meteorological  
705 characteristics (Table 1). However, short-term catchment responses (such as storm-induced  
706 peak flows and related changes in hydrochemistry) were difficult to be captured by this  
707 sampling approach. Furthermore, two years of field data are probably not sufficient to capture



708 all hydrological conditions and catchment responses to specific meteorological conditions. In  
709 this regards, long-term studies may have better chances in capturing the temporal variability  
710 of hydrochemical responses (Thies et al., 2007). In this context, sampling approaches might  
711 need to become more complex in future to unravel further process understanding of  
712 glacierized catchments.

713

## 714 **5 Conclusions**

715 Our results highlight the complex hydrochemical responses of mountain glacierized  
716 catchments at different temporal and spatial scales. To our knowledge, only few studies  
717 investigated the impact of controlling factors on stream water hydrochemistry by using nivo-  
718 meteorological indicators and multi-tracer data, which we recommend to establish as  
719 prerequisite for studies in other glacierized catchments.

720 The main results of this study can be summarized as follows:

- 721 • Hydrometric and geochemical dynamics were controlled by an interplay of  
722 meteorological conditions and the geological heterogeneity. The majority of the  
723 variance (PC1: 36.3 %) was explained by heavy metal concentrations (such as Al, V,  
724 Cr, Ni, Zn, Cd, Pb), associated with atmospheric deposition on the snowpack and  
725 release through snowmelt. Remaining variance (PC2: 16.3 %) resulted both from the  
726 presence of a bedrock-specific geochemical signature (As and Sr concentrations) and  
727 the role of snowmelt contribution.
- 728 • The isotopic composition of rock glacier outflow was relatively similar to the  
729 composition of glacier melt whereas high concentrations of As and Sr may more likely  
730 result from bedrock weathering.
- 731 • At the monthly scale for different sub-catchments (spatial scale: 0.05 – 130 km<sup>2</sup>), both  
732  $\delta^{18}\text{O}$  and EC revealed complex spatial and temporal dynamics such as contrasting EC  
733 gradients during baseflow conditions and melting periods.
- 734 • At the daily scale for the entire study area (spatial scale: 130 km<sup>2</sup>), we observed strong  
735 relationships of hydrochemical variables, with mainly discharge and EC exhibiting a  
736 strong monthly relationship. This was characterised by a hysteretic-like pattern,  
737 determined by highest EC and lowest discharge during baseflow conditions on the one  
738 hand and maximum EC dilution due to highest discharge during a summer storm.





739       • Main drivers of EC and  $\delta^2\text{H}$  variability were the nivo-meteorological indicators  $T_{\text{max}3\text{d}}$ ,  
740        $G_{\text{max}1\text{d}}$  and  $\Delta\text{SD}_{15\text{d}}$ .  $\Delta\text{SD}$  was found to be the most sensitive variable to different  
741       temporal lengths (3d, 5d, and 15d) and  $G_{\text{max}1\text{d}}$  resulted in the most pronounced EC  
742       dilution and isotopic depletion.

743       Finally, this study may support future classifications of glacierized catchments according to  
744       their hydrochemical response under different catchment conditions or the prediction of  
745       appropriate end-member signatures for hydrograph separation being valid at longer time  
746       scales.

## 747       **6 Data availability**

748       Hydrometeorological data are available upon request at the Hydrographic Office of the  
749       Autonomous Province of Bozen-Bolzano. Tracer data used in this study are freely available  
750       by contacting the authors.

751

## 752       **7 Acknowledgements**

753       This research is part of the GLACIALRUN project and funded by the foundation of the Free  
754       University of Bozen-Bolzano and supported by the project "Parco Tecnologico - Tecnologie  
755       ambientali".

756       The authors thank Andrea Ruecker, Alex Boninsegna, Raffael Foffa, and Michiel Blok for  
757       their field assistance. Giulia Zuecco and Luisa Pianezzola are thanked for the isotopic analysis  
758       at TESAF, University of Padova and Christian Ceccon for the isotopic analysis in the  
759       laboratory of the Free University of Bozen-Bolzano. We also thank Giulio Voto at  
760       EcoResearch s.r.l. (Bozen/Bolzano) for the element analysis. We appreciate the helpful  
761       support for the geological interpretation by Volkmar Mair. We acknowledged the project  
762       AQUASED, whose instrumentation infrastructure we could use. Furthermore, we thank the  
763       Hydrographic Office and the Department of Hydraulic Engineering of the Autonomous  
764       Province of Bozen-Bolzano for providing meteorological and hydrometric data. We  
765       acknowledge the Forestry Commission Office Prat, the National Park Stilfser Joch / Passo  
766       Stelvio, and the Cable car Sulden GmbH for their logistical support and helpful advices.

767



768 **8 References**

- 769 Anderson, S.P., Drever, J.I., and Humphrey, N.F.: Chemical weathering in glacial  
770 environments, *Geology*, 25, 399–402, 1997.
- 771 Andreatta, C.: Polymetamorphose und Tektonik in der Ortlergruppe. - *N. Jb. Mineral. Mh.*  
772 *Stuttgart*, 1, 13–28, 1952.
- 773 Anslow, F. S., Hostetler, S., Bidlake, W. R. and Clark, P. U.: Distributed energy balance  
774 modeling of South Cascade Glacier, Washington and assessment of model uncertainty,  
775 *J. Geophys. Res.*, 113(F02019), 1–18, doi:10.1029/2007JF000850, 2008.
- 776 Auer, A. H.: The rain versus snow threshold temperatures, *Weatherwise*, 27, 67, 1974.
- 777 Baraer, M., McKenzie, J., Mark, B. G., Gordon, R., Bury, J., Condom, T., Gomez, J., Knox,  
778 S. and Fortner, S. K.: Contribution of groundwater to the outflow from ungauged  
779 glacierized catchments: a multi-site study in the tropical Cordillera Blanca, Peru,  
780 *Hydrol. Process.*, 29, 2561–2581, doi: 10.1002/hyp.10386, 2015.
- 781 Beniston, M.: Climatic change in mountain regions: a review of possible impacts; *Clim.*  
782 *Change*. 59, 5–31, doi: 10.1023/A: 1024458411589, 2003.
- 783 Beniston, M.: Mountain weather and climate: A general overview and a focus on climatic  
784 change in the Alps; *Hydrobiologia*, 562, 3–16, doi: 10.1007/s10750-005-1802-0, 2006.
- 785 Beniston, M., and Stoffel, M.: Assessing the impacts of climatic change on mountain water  
786 resources, *Sci. Total Environ.* 493, 1129–37, doi: 10.1016/j.scitotenv.2013.11.122,  
787 2014.
- 788 Boeckli, L., Brenning, A., Gruber, S., and Noetzli, J.: A statistical approach to modelling  
789 permafrost distribution in the European Alps or similar mountain ranges, *Cryosph.*, 6,  
790 125–140, doi: 10.5194/tc-6-125-2012, 2012.
- 791 Braithwaite, R. J.: On glacier energy balance, ablation, and air temperature, *J. Glaciol.*, 27,  
792 381–391, 1981.
- 793 Brown, G. H.: Glacier meltwater hydrochemistry, *Appl. Geochemistry*, 17(7), 855–883,  
794 doi:10.1016/S0883-2927(01)00123-8, 2002.



- 795 Brown, G.H., and Fuge, R.: Trace element chemistry of glacial meltwaters in an Alpine  
796 headwater catchment, *Hydrol. Water Resour. Ecol. Headwaters*, 2, 435–442, 1998.
- 797 Brown, G. H., Tranter, M., and Sharp, M.: Subglacial chemical erosion—seasonal variations  
798 in solute provenance, Haut Glacier d'Arolla, Switzerland, *Ann. Glaciol.*, 22, 25-31,  
799 1996.
- 800 Brown, L.E., Hannah, D.M., Milner, A.M., Soulsby, C., Hodson, A.J., and Brewer, M.J.:  
801 Water source dynamics in a glacierized alpine river basin (Taillon-Gabiétous, French  
802 Pyrénées), *Water Resour. Res.*, 42, doi: 10.1029/2005WR004268, 2006.
- 803 Brugnara, Y., Brunetti, M., Maugeri, M., Nanni, T. and Simolo, C.: High-resolution analysis  
804 of daily precipitation trends in the central Alps over the last century, *Int. J. Climatol.*,  
805 32(9), 1406–1422, doi:10.1002/joc.2363, 2012.
- 806 Carey, S. K., Boucher, J. L. and Duarte, C. M.: Inferring groundwater contributions and  
807 pathways to streamflow during snowmelt over multiple years in a discontinuous  
808 permafrost subarctic environment (Yukon, Canada), *Hydrogeol. J.*, 21, 67–77, doi:  
809 10.1007/s10040-012-0920-9, 2013.
- 810 Carrillo, G., Troch, P.A., Sivapalan, M., Wagener, T., Harman, C., Sawicz, K.: Catchment  
811 classification: hydrological analysis of catchment behavior through process-based  
812 modeling along a climate gradient, *Hydrol. Earth Syst. Sci.*, 15, 3411–3430,  
813 doi:10.5194/hess-15-3411-2011, 2011.
- 814 Carturan, L., Zuecco, G., Seppi, R., Zanoner, T., Borga, M., Carton, A. and Dalla Fontana, G.:  
815 Catchment-Scale Permafrost Mapping using Spring Water Characteristics, *Permafr.*  
816 *Periglac. Process.*, 27(3), 253–270, doi:10.1002/ppp.1875, 2016.
- 817 Chiogna, G., Santoni, E., Camin, F., Tonon, A., Majone, B., Trenti, A. and Bellin, A.: Stable  
818 isotope characterization of the Vermigliana catchment, *J. Hydrol.*, 509, 295–305,  
819 doi:10.1016/j.jhydrol.2013.11.052, 2014.
- 820 Clark, I.D., Lauriol, B., Harwood, L., Marschner, M.: Groundwater contributions to discharge  
821 in a permafrost setting, Big Fish River, N.W.T., Canada, *Arct. Antarct. Alp. Res.*, 33,  
822 62–69, 2001.
- 823 Colbeck, S.: A theory of water percolation in snow, *J. Glaciol.*, 11, 369–385, 1972.



- 824 Coléou, C., and Lesaffre, B.: Irreducible water saturation in snow: experimental results in a  
825 cold laboratory, *Ann. Glaciol.*, 26, 64–68, 1998.
- 826 Colombo, N., Salerno, F., Gruber, S., Freppaz, M., Williams, M., Fratianni, S. and Giardino,  
827 M.: Review: Impacts of permafrost degradation on inorganic chemistry of surface  
828 fresh water, *Glob. Planet. Change*, 162, 69–83, doi:10.1016/j.gloplacha.2017.11.017,  
829 2017.
- 830 Cook, S.J., and Swift, D.A.: Subglacial basins: Their origin and importance in glacial systems  
831 and landscapes, *Earth-Science Rev.* 115, 332–372, doi:  
832 10.1016/j.earscirev.2012.09.009, 2012.
- 833 Cortés, G., Vargas, X., McPhee, J.: Climatic sensitivity of streamflow timing in the  
834 extratropical western Andes Cordillera, *J. Hydrol.*, 405, 93–109, doi:  
835 10.1016/j.jhydrol.2011.05.013, 2011.
- 836 Craig, H.: Standard for reporting concentrations of deuterium and oxygen-18 in natural  
837 waters, *Science*, 133, 1833-1834, 1961.
- 838 DeBeer, C.M., and Pomeroy, J.W.: Simulation of the snowmelt runoff contributing area in a  
839 small alpine basin, *Hydrol. Earth Syst. Sci.*, 14, 1205–1219, doi: 10.5194/hess-14-  
840 1205-2010, 2010.
- 841 Devito, K., Creed, I., Gan, T., Mendoza, C., Petrone, R., Silins, U., and Smerdon, B.: A  
842 framework for broad-scale classification of hydrologic response units on the Boreal  
843 Plain: Is topography the last thing to consider? *Hydrol. Process.*, 19, 1705–1714,  
844 doi:10.1002/hyp.5881, 2005.
- 845 Dye, D.G.: Variability and trends in the annual snow-cover cycle in Northern Hemisphere  
846 land areas, 1972-2000, *Hydrol. Process.*, 16, 3065–3077, doi:10.1002/hyp.1089, 2002.
- 847 Engel, M., Penna, D., Bertoldi, G., Dell’Agnese, A., Soulsby, C., and Comiti, F.: Identifying  
848 run-off contributions during melt-induced runoff events in a glacierized Alpine  
849 catchment, *Hydrol. Process.*, 30, 343–364, doi:10.1002/hyp.10577, 2016.
- 850 Engel, M., Penna, D., Tirlir, W., and Comiti F.: Multi-Parameter-Analyse zur  
851 Charakterisierung von Landschaftsmerkmalen innerhalb eines experimentellen  
852 Messnetzes im Hochgebirge, In M. Casper et al. (Eds.): *Den Wandel Messen –*



- 853 Proceedings Tag der Hydrologie 2017, Forum für Hydrologie und  
854 Wasserbewirtschaftung, Vol. 38, 293 – 299, 2017.
- 855 Engel, M., Brighenti S., Bruno MC., Tolotti M., Comiti F.: Multi-tracer approach for  
856 characterizing rock glacier outflow, 5th European Conference on Permafrost,  
857 Chamonix-Mont Blanc, 2018.
- 858 Epstein, S. and Mayeda, T.: Variation of  $\delta^{18}\text{O}$  content in waters from natural sources,  
859 Geochim. Cosmochim. Ac., 4, 213–224, 1953.
- 860 Farvolden, R.N., Geological controls on ground-water storage and base flow, J. Hydrol., 1,  
861 219–249, 1963.
- 862 Freyberg, J. Von, Studer, B. and Kirchner, J. W.: A lab in the field: high-frequency analysis  
863 of water quality and stable isotopes in stream water and precipitation, Hydrol. Earth  
864 Syst. Sci., 21, 1721–1739, doi:10.5194/hess-21-1721-2017, 2017.
- 865 Fischer, B. M. C., Rinderer, M., Schneider, P., Ewen, T. and Seibert, J.: Contributing sources  
866 to baseflow in pre-alpine headwaters using spatial snapshot sampling, Hydrol.  
867 Process., 29, 5321–5336, doi:10.1002/hyp.10529, 2015.
- 868 Gabrielli, P., Cozzi, G., Torcini, S., Cescon, P., Barbante, C.: Source and origin of  
869 atmospheric trace elements entrapped in winter snow of the Italian Eastern Alps,  
870 Atmos. Chem. Phys. Discuss., 6, 8781–8815, doi: 10.5194/acpd-6-8781-2006, 2006.
- 871 Galos, S.P., Klug, C., Prinz, R., Rieg, L., Sailer, R., Dinale, R., Kaser, G.: Recent glacier  
872 changes and related contribution potential to river discharge in the Vinschgau / Val  
873 Venosta, Italian Alps, Geogr. Fis. e Din. Quat., 38, 143–154,  
874 doi:10.4461/GFDQ.2015.38.13, 2015.
- 875 Gat, J. R. and Carmi, I.: Evolution of the isotopic composition of atmospheric waters in the  
876 Mediterranean Sea area, J. Geophys. Res., 75, 3039–3048, 1970.
- 877 Genereux, D.: Quantifying uncertainty in tracer-based hydrograph separations, Water Resour.  
878 Res., 34, 915–919, 1998.
- 879 Gordon, R. P., Lautz, L. K., McKenzie, J. M., Mark, B. G., Chavez, D. and Baraer, M.:  
880 Sources and pathways of stream generation in tropical proglacial valleys of the  
881 Cordillera Blanca, Peru, J. Hydrol., 522, 628–644, doi: 10.1016/j.jhydrol.2015.01.013



- 882           2015.
- 883   Gruber, S., Fleiner, R., Guegan, E., Panday, P., Schmid, M.O., Stumm, D., Wester, P., Zhang,  
884           Y., and Zhao, L.: Review article: Inferring permafrost and permafrost thaw in the  
885           mountains of the Hindu Kush Himalaya region, *Cryosph*, 11, 81–99, doi:10.5194/tc-  
886           11-81-2017, 2017.
- 887   Guo, B., Liu, Y., Zhang, F., Hou, J. and Zhang, H.: Heavy metals in the surface sediments of  
888           lakes on the Tibetan Plateau , China, *Environ. Sci. Pollut. Res.*, 25(4), 3695–3707, doi:  
889           10.1007/s11356-017-0680-0, 2017.
- 890   Hannah, D.M., Gurnell, A.M., and McGregor, G.R.: A methodology for investigation of the  
891           seasonal evolution in proglacial hydrograph form, *Hydrol. Process.*, 13, 2603–2621,  
892           doi: 10.1002/(SICI)1099-1085(199911)13:16<2603::AID-HYP936>3.0.CO;2-5, 1999.
- 893   Harris, C., Haeberli, W., Mühlh, D.Vonder, and King, L.: Permafrost monitoring in the high  
894           mountains of Europe: the PACE project in its global context, *Permafr. Periglac.*  
895           *Process.*, 12, 3–11, doi:10.1002/ppp, 2001.
- 896   Heidbüchel, I., Troch, P. A. and Lyon, S. W.: Separating physical and meteorological controls  
897           of variable transit times in zero-order catchments, *Water Resour. Res.*, 49(11), 7644–  
898           7657, doi:10.1002/2012WR013149, 2013.
- 899   Hindshaw, R.S., Tipper, E.T., Reynolds, B.C., Lemarchand, E., Wiederhold, J.G.,  
900           Magnusson, J., Bernasconi, S.M., Kretzschmar, R., and Bourdon, B.: Hydrological  
901           control of stream water chemistry in a glacial catchment (Damma Glacier,  
902           Switzerland), *Chem. Geol.*, 285, 215–230, doi:10.1016/j.chemgeo.2011.04.012, 2011.
- 903   Hodgkins, R.: Seasonal evolution of meltwater generation, storage and discharge at a non-  
904           temperate glacier in Svalbard, *Hydrol. Process.*, 15, 441–460, 10.1002/hyp.160, 2001.
- 905   International Atomic Energy Agency: IAEA/GNIP precipitation sampling guide V2.02  
906           September 2014, International Atomic Energy Agency, Vienna, Austria, pp. 19, 2014.
- 907   IPCC, 2013. Climate Change 2013: The Physical Science Basis. Contribution of Working  
908           Group I to the Fifth Assessment Report of the Intergovernmental Panel on Climate  
909           Change. In: Stocker, T.F., Qin, D., Plattner, G.-K., Tignor, M., Allen, S.K., Boschung,  
910           J., Nauels, A., Xia, Y., Bex, V., Midgley, P.M., (Eds.), International Organization for



- 911 Standardization Standard Atmosphere, ISO 2533, Cambridge University Press,  
912 Cambridge, United Kingdom and New York, NY, USA, 1535, pp. ISO, 1975.
- 913 Kaser, G., Grosshauser, M., and Marzeion, B.: Contribution potential of glaciers to water  
914 availability in different climate regimes, in: Proceedings of the National Academy of  
915 Sciences of the United States of America, 20223–20227,  
916 doi:10.1073/pnas.1008162107, 2010.
- 917 Katsuyama, M., Tani, M., and Nishimoto S.: Connection between streamwater mean  
918 residence time and bedrock groundwater recharge/discharge dynamics in weathered  
919 granite catchments, *Hydrol. Process.*, 24, 2287–2299, doi:10.1002/hyp.7741, 2010.
- 920 Kirchner, J.W.: Catchments as simple dynamical systems: Catchment characterization,  
921 rainfall-runoff modeling, and doing hydrology backward, *Water Resour. Res.*, 45,  
922 W02429, doi:10.1029/2008WR006912, 2009.
- 923 Kong, Y., and Pang, Z.: Evaluating the sensitivity of glacier rivers to climate change based on  
924 hydrograph separation of discharge, *J. Hydrol.* 434–435, 121–129,  
925 doi:10.1016/j.jhydrol.2012.02.029, 2012.
- 926 Krainer, K., and Mostler, W.: Hydrology of active rock glaciers: examples from the Austrian  
927 Alps, *Arct. Antarct. Alp. Res.*, 34, 142–149, 2002.
- 928 Krainer, K., Mostler, W., and Spötl, C.: Discharge from active rock glaciers, Austrian Alps: a  
929 stable isotope approach, *Austrian J. Earth Sc.*, 100, 102–112, 2007.
- 930 Krainer, K., Bressan, D., Dietre, B., Haas, J.N., Hajdas, I., Lang, K., Mair, V., Nickus, U.,  
931 Reidl, D., Thies, H., and Tonidandel, D.: A 10,300-year-old permafrost core from the  
932 active rock glacier Lazaun, southern Ötztal Alps (South Tyrol, northern Italy), *Quat.*  
933 *Res.*, 83, 324–335, doi:10.1016/j.yqres.2014.12.005, 2015.
- 934 Lewis, T., Lafrenière, M.J., and Lamoureux, S.F.: Hydrochemical and sedimentary responses  
935 of paired High Arctic watersheds to unusual climate and permafrost disturbance, Cape  
936 Bounty, Melville Island, Canada, *Hydrol. Process.*, 26, 2003–2018,  
937 doi:10.1002/hyp.8335, 2012.



- 938 Liu, F., Williams, M.W., and Caine, N.: Source waters and flow paths in an alpine catchment,  
939 Colorado Front Range, United States, *Water Resour. Res.*, 40,  
940 doi:10.1029/2004WR003076, 2004.
- 941 Longinelli, A. and Selmo, E.: Isotopic composition of precipitation in Italy: a first overall  
942 map, *J. Hydrol.*, 270, 75–88, 2003.
- 943 Mair, V.: Die Kupferbergbaue von Stilfs, Eysrs und Klausen, *Der Stoansucher* 10 (1), 38-44,  
944 1996.
- 945 Mair, V., Lorenz, D., and Eschgfäller, M.: Mineralienwelt Südtirol. Verlag Tappeiner, Lana  
946 (BZ), 215 S., 2009.
- 947 Mair, V., Müller, J.P., and Reisigl, H.: Leben an der Grenze. Konsortium Nationalpark  
948 Stilfserjoch – Gemeinde Stilfs, Glurns (BZ), 120 S., 2002.
- 949 Mair, V., Nocker, C., and Tropper, P.: Das Ortler-Campo Kristallin in Südtirol, *Mitt. Österr.*  
950 *Mineral. Ges.*, 153, 219–240, 2007.
- 951 Mair, V., Zischg, A., Lang, K., Tonidandel, D., Krainer, K., Kellerer-Pirklbauer, A., Deline,  
952 P., Schoeneich, P., Cremonese, E., Pogliotti, P., Gruber, S. and Böckli, L.: PermaNET  
953 - Permafrost Long-term Monitoring Network. Synthesis report. INTERPRAEVENT  
954 Journal series 1, Report 3. Klagenfurt, 2011.
- 955 Marsh, P., and J. W. Pomeroy, Meltwater fluxes at an arctic forest- tundra site, *Hydrol.*  
956 *Processes*, 10, 1383-1400, 1996.
- 957 Maurya, A.S., Shah, M., Deshpande, R.D., Bhardwaj, R.M., Prasad, A., and Gupta, S.K.:  
958 Hydrograph separation and precipitation source identification using stable water  
959 isotopes and conductivity: River Ganga at Himalayan foothills, *Hydrol. Process.*, 25,  
960 1521–1530, doi:10.1002/hyp.7912, 2011.
- 961 McClymont, A.F., Hayashi, M., Bentley, L.R., Muir, D., and Ernst, E.: Groundwater flow  
962 and storage within an alpine meadow-talus complex, *Hydrol. Earth Syst. Sci.*, 14, 859–  
963 872, doi:10.5194/hess-14-859-2010, 2010.
- 964 Milly, P.C.D., Betancourt, J., Falkenmark, M., Hirsch, R.M., Kundzewicz, Z.W., Lettenmaier,  
965 D.P., Stouffer, R.J.: Stationarity is dead—whither water management? *Science*, 319,  
966 573–574, doi:10.1126/science.1151915, 2008.





- 967 Milner, A., Brown, L.E., and Hannah, D.M.: Hydroecological response of river systems to  
968 shrinking glaciers, *Hydrol. Process.* 23, 62–77, doi:10.1002/hyp.7197 2009.
- 969 Montrasio, A. Berra, F., Cariboni, M., Ceriani, M., Deichmann, N., Ferliga, C., Gregnanin,  
970 A., Guerra, S., Guglielmin, M., Jadoul, F., Lonhghin, M., Mair, V., Mazzoccola, D.,  
971 Sciesa, E. & Zappone, A.: Note illustrative della Carta geologica d'Italia alla scala  
972 1:50.000 Foglio 024 Bormio. ISPRA, Servizio Geologico D'Italia; System Cart, Roma  
973 2012, 150 S., 2012.
- 974 Moore, R. D., Fleming, S. W., Menounos, B., Wheate, R., Fountain, A., Stahl, K., Holm, K.  
975 and Jakob, M.: Glacier change in western North America: influences on hydrology,  
976 geomorphic hazards and water quality, *Hydrol. Process.*, 23, 42–61,  
977 10.1002/hyp.7162, 2009.
- 978 Mutzner, R., Weijs, S. V., Tarolli, P., Calaf, M., Oldroyd, J., and Parlange, M.B.: Controls on  
979 the diurnal streamflow cycles in two subbasins of an alpine headwater catchment,  
980 *Water Resour. Res.*, 51, 3403–3418, doi:10.1016/0022-1694(68)90080-2, 2015.
- 981 Nickus U., Krainer K., Thies H. and Tolotti M.: Blockgletscherabflüsse am Äußeren  
982 Hochebenkar –Hydrologie, Wasserchemie und Kieselalgen. In: Schallart N. &  
983 Erschbamer B. (eds), *Forschung am Blockgletscher, Methoden und Ergebnisse*. Alpine  
984 Forschungstelle Obergurgl, Innsbruck University Press, Innsbruck (A), 4: 117-134.  
985 ISBN 978-3-902936-58-5, 2015.
- 986 Nordstrom, D. K. Hydrogeochemical processes governing the origin, transport and fate of  
987 major and trace elements from mine wastes and mineralized rock to surface waters,  
988 *Appl. Geochem.*, 26, 1777–1791, 2011.
- 989 Onda, Y., Komatsu, Y., Tsujimura, M., and Fujihara, J. I.: The role of subsurface runoff  
990 through bedrock on storm flow generation, *Hydrol. Processes*, 15, 1693–1706,  
991 doi:10.1002/hyp.234, 2001.
- 992 Penna, D., Stenni, B., Šanda, M., Wrede, S., Bogaard, T.A., Gobbi, A., Borga, M., Fischer,  
993 B.M.C., Bonazza, M., and Chárová, Z.: On the reproducibility and repeatability of  
994 laser absorption spectroscopy measurements for  $\delta^2\text{H}$  and  $\delta^{18}\text{O}$  isotopic analysis,  
995 *Hydrol. Earth Syst. Sci.*, 14, 1551–1566, doi:10.5194/hess-14-1551-2010, 2010.



- 996 Penna, D., Stenni, B., Šanda, M., Wrede, S., Bogaard, T.A., Michelini, M., Fischer, B.M.C.,  
997 Gobbi, A., Mantese, N., Zuecco, G., Borga, M., Bonazza, M., Sobotková, M.,  
998 Čejková, B. and Wassenaar, L.I.: Technical Note: Evaluation of between-sample  
999 memory effects in the analysis of  $\delta^2\text{H}$  and  $\delta^{18}\text{O}$  of water samples measured by laser  
1000 spectrometers, *Hydrol. Earth Syst. Sci.*, 16, 3925–3933, doi:10.5194/hess-16-3925-  
1001 2012, 2012.
- 1002 Penna, D., Engel, M., Mao, L., Agnese, A. D., Bertoldi, G. and Comiti, F.: Tracer-based  
1003 analysis of spatial and temporal variations of water sources in a glacierized catchment,  
1004 *Hydrol. Earth Syst. Sci.*, 18, 5271–5288, 10.5194/hess-18-5271-2014, 2014.
- 1005 Penna, D., Engel, M., Bertoldi, G., and Comiti, F.: Towards a tracer-based conceptualization  
1006 of meltwater dynamics and streamflow response in a glacierized catchment, *Hydrol.*  
1007 *Earth Syst. Sci.*, 21, 23–41, 10.5194/hess-21-23-2017, 2017.
- 1008 R Core Team: R: A Language and Environment for Statistical Computing. R Foundation for  
1009 Statistical Computing, Vienna, Austria, 2016.
- 1010 Ragettli, S., Immerzeel, W.W., and Pellicciotti, F.: Contrasting climate change impact on  
1011 river flows from high-altitude catchments in the Himalayan and Andes Mountains,  
1012 *Proc. Natl. Acad. Sci.*, 113, 9222–9227, doi:10.1073/pnas.1606526113, 2016.
- 1013 Ragettli, S., and Pellicciotti, F.: Calibration of a physically based, spatially distributed  
1014 hydrological model in a glacierized basin: On the use of knowledge from  
1015 glaciometeorological processes to constrain model parameters, *Water Resour. Res.*,  
1016 48, 1–20, doi:10.1029/2011WR010559, 2012.
- 1017 Rinaldo, A., Benettin, P., Harman, C.J., Hrachowitz, M., McGuire, K.J., Velde, Y. Van Der,  
1018 Bertuzzo, E., Botter, G.: Storage selection functions: A coherent framework for  
1019 quantifying how catchments store and release water and solutes, *Water Resources Res.*  
1020 51, doi:10.1002/2015WR017273, 2015.
- 1021 Rogger, M., Chirico, G.B., Hausmann, H., Krainer, K., Brückl, E., Stadler, P., Blöschl, G.:  
1022 Impact of mountain permafrost on flow path and runoff response in a high alpine  
1023 catchment, *Water Resour. Res.*, 53 (2), 1288–1308, 2017.



- 1024 Roy, J.W., and Hayashi, M.: Multiple, distinct groundwater flow systems of a single moraine–  
1025 talus feature in an alpine watershed, *J. Hydrol.*, 373, 139–150, doi:  
1026 10.1016/j.jhydrol.2009.04.018, 2009.
- 1027 Rutter, N., Hodson, A., Irvine-Fynn, T., and Solås, M.K.: Hydrology and hydrochemistry of a  
1028 deglaciating high-Arctic catchment, Svalbard, *J. Hydrol.* 410, 39–50,  
1029 doi:10.1016/j.jhydrol.2011.09.001, 2011.
- 1030 Schaefli, B., Maraun, D. and Holschneider, M.: What drives high flow events in the Swiss  
1031 Alps? Recent developments in wavelet spectral analysis and their application to  
1032 hydrology, *Adv. Water Resour.*, 30, 2511–2525, doi:10.1016/j.advwatres.2007.06.004,  
1033 2007.
- 1034 Schmieder, J., Marke, T., and Strasser, U. Tracerhydrologische Untersuchungen im Rofental  
1035 (Ötztaler Alpen / Österreich). *Innsbrucker Jahresbericht, Institut für Geographie der*  
1036 *Universität Innsbruck*, 109 – 120, 2017.
- 1037 Schwarb, M.: *The Alpine Precipitation Climate*. Swiss Federal Institut of Technology Zurich,  
1038 2000.
- 1039 Shevchenko, V. P., Pokrovsky, O. S., Vorobyev, S. N., Krickov, I. V., Manasypov, R. M.,  
1040 Politova, N. V., Kopysov, S. G., Dara, O. M., Auda, Y., Shirokova, L. S.,  
1041 Kolesnichenko, L. G., et al.: Impact of snow deposition on major and trace element  
1042 concentrations and fluxes in surface waters of Western Siberian Lowland, *Hydrol.*  
1043 *Earth Syst. Sci.*, 21, 5725–5746, doi:10.5194/hess-2016-578, 2016.
- 1044 Sicart, J.E., Pomeroy, J.W., Essery, R.L.H., Bewley, D.: Incoming longwave radiation to  
1045 melting snow: Observations, sensitivity and estimation in northern environments.  
1046 *Hydrol. Process.* 20, 3697–3708, doi:10.1002/hyp.6383, 2006.
- 1047 Sicart, J. E., Hock, R. and Six, D.: Glacier melt, air temperature, and energy balance in  
1048 different climates: The Bolivian Tropics, the French Alps, and northern Sweden, *J.*  
1049 *Geophys. Res.*, 113, 1–11, doi: 10.1029/2008JD010406, 2008.
- 1050 Singh, P., Haritashya, U.K., Ramasastri, K.S., and Kumar, N.: Diurnal variations in discharge  
1051 and suspended sediment concentration, including runoff-delaying characteristics, of



- 1052 the Gangotri Glacier in the Garhwal Himalayas, *Hydrol. Process.*, 19, 1445–1457,  
1053 doi:10.1002/hyp.5583 2005.
- 1054 Sivapalan, M.: Prediction in ungauged basins: a grand challenge for theoretical hydrology,  
1055 *Hydrol. Process.* 17, 3163–3170, doi:10.1002/hyp.5155, 2003
- 1056 Sklash, M. G., R. N. Farvolden, and Fritz, P.: A conceptual model of watershed response to  
1057 rainfall, developed through the use of oxygen-18 as a natural tracer, *Can. J. Earth Sci.*,  
1058 13, 271–283, 1976.
- 1059 Soulsby, C., Tetzlaff, D., Dunn, S. M. and Waldron, S.: Scaling up and out in runoff process  
1060 understanding: Insights from nested experimental catchment studies, *Hydrol. Process.*,  
1061 20, 2461–2465, doi: 10.1002/hyp.6338, 2006a.
- 1062 Soulsby, C., Tetzlaff, D., Rodgers, P., Dunn, S. and Waldron, S.: Runoff processes, stream  
1063 water residence times and controlling landscape characteristics in a mesoscale  
1064 catchment: An initial evaluation, *J. Hydrol.*, 325, 197–221, doi:  
1065 10.1016/j.jhydrol.2005.10.024, 2006b.
- 1066 Sprenger, M., Leistert, H., Gimbel, K. and Weiler, M.: Illuminating hydrological processes at  
1067 the soil-vegetation-atmosphere interface with water stable isotopes, *Rev. Geophys.*,  
1068 54, 674–704, doi:10.1002/2015RG000515, 2016.
- 1069 Stingl, V. and Mair, V.: An introduction to the geology of South Tyrol. Autonome Provinz  
1070 Bozen, Amt für Geologie und Baustoffprüfung, Kardaun (BZ), 80 S., 2005.
- 1071 Tetzlaff, D., Buttle, J., Carey, S.K., McGuire, K., Laudon, H., and Soulsby, C.: Tracer-based  
1072 assessment of flow paths, storage and runoff generation in northern catchments: a  
1073 review, *Hydrol. Process.*, 29, 3475–3490, doi: 10.1002/hyp.10412, 2014.
- 1074 Thies, H., Nickus, U., Mair, V., Tessadri, R., Tait, D., Thaler, B. and Psenner, R.: Unexpected  
1075 response of high Alpine Lake waters to climate warming, *Environ. Sci. Technol.*, 41,  
1076 7424–9, 2007.
- 1077 Thies, H., Nickus, U., Tolotti, M., Tessadri, R., Krainer, K., Evidence of rock glacier melt  
1078 impacts on water chemistry and diatoms in high mountain streams, *Cold Reg. Sci.*  
1079 *Technol.*, 96, 77–85, doi:10.1016/j.coldregions.2013.06.006, 2013.



- 1080 Troch, P.A., Lahmers, T., Meira, A., Mukherjee, R., Pedersen, J.W., Roy, T., and Valdés-  
1081 Pineda, R.: Catchment coevolution: A useful framework for improving predictions of  
1082 hydrological change? *Water Resour. Res.*, 4903–4922, doi:10.1002/2015WR017032,  
1083 2015.
- 1084 Uhlenbrook, S. and Hoeg, S.: Quantifying uncertainties in tracer-based hydrograph  
1085 separations : a case study for two-, three- and five-component hydrograph separations  
1086 in a mountainous catchment, *Hydrol. Process.*, 17, 431–453, doi:10.1002/hyp.1134,  
1087 2003.
- 1088 U.S. Army Corps of Engineers: Summary Report of the Snow Investigations, Snow  
1089 Hydrology , North Pacific Division, Portland, Oregon, 1956.
- 1090 Vaughn, B. H. and Fountain, A. G.: Stable isotopes and electrical conductivity as keys to  
1091 understanding water pathways and storage in South Cascade Glacier, Washington,  
1092 USA, *Ann. Glaciol.*, 40, 107–112, doi: 10.3189/172756405781813834, 2005.
- 1093 Vincent, C. and Six, D.: Relative contribution of solar radiation and temperature in enhanced  
1094 temperature-index melt models from a case study at Glacier de Saint-Sorlin, France,  
1095 *Ann. Glaciol.*, 54(63), 11–17, doi:10.3189/2013AoG63A301, 2013.
- 1096 Viviroli, D., Archer, D.R., Buytaert, W., Fowler, H.J., Greenwood, G.B., Hamlet, A. F.,  
1097 Huang, Y., Koboltschnig, G.R., Litaor, M.I., López-Moreno, J.I., Lorentz, S.,  
1098 Schädler, B., Schreier, H., Schwaiger, K., Vuille, M., and Woods, R.: Climate change  
1099 and mountain water resources: overview and recommendations for research,  
1100 management and policy, *Hydrol. Earth Syst. Sci.*, 15, 471–504, doi:10.5194/hess-15-  
1101 471-2011, 2011.
- 1102 Weiler, M., Seibert, J. and Stahl, K.: Magic components - why quantifying rain, snow- and  
1103 icemelt in river discharge isn't easy, *Hydrol. Process.*, doi:10.1002/hyp.11361, 2017.
- 1104 Williams, M.W., Knauf, M., Caine, N., Liu, F., Verplanck, P.L.: Geochemistry and source  
1105 waters of rock glacier outflow, Colorado Front Range, *Permafr. Periglac. Process.*, 17,  
1106 13–33, doi:10.1002/ppp.535, 2006.



- 1107 Williams, M.W., Hood, E., Molotch, N.P., Caine, N., Cowie, R., and Liu, F.: The ‘teflon  
1108 basin’ myth: hydrology and hydrochemistry of a seasonally snow-covered catchment,  
1109 Plant Ecol. Divers., 8, 639–661, doi:10.1080/17550874.2015.1123318,2015.
- 1110 Wolfe, P.M. and English, M.C.: Hydrometeorological relationships in a glacierized catchment  
1111 in the Canadian high Arctic, Hydrol. Process., 9, 911–921, 10.1002/hyp.3360090807,  
1112 1995.
- 1113 Xing, B., Liu, Z., Liu, G., Zhang, J.: Determination of runoff components using path analysis  
1114 and isotopic measurements in a glacier-covered alpine catchment (upper Hailuogou  
1115 Valley) in southwest China, Hydrol. Process., 29, 3065–3073, doi:10.1002/hyp.10418,  
1116 2015.
- 1117 Zhou, S., Wang, Z. and Joswiak, D. R.: From precipitation to runoff: stable isotopic  
1118 fractionation effect of glacier melting on a catchment scale, Hydrol. Process., 28,  
1119 3341–3349, doi: 10.1002/hyp.9911, 2014.
- 1120 Zuzel, J.F., and Cox, L.M.: Relative importance of meteorological variables in snowmelt,  
1121 Water Resour. Res., 11, 174–176, 1975.  
1122



1123 Table 1. Meteorological characteristics of the weather station Madritsch/Madriccio 2.825 m  
1124 a.s.l. in 2014 and 2015.

Date	2014	2015
Precipitation (total / rain / snow) (mm y <sup>-1</sup> )*	1284/704/579	961/637/323
Mean annual air temperature (°C)	-1.4	-0.8
Days with snow cover > 10cm	270	222
Maximum snow depth (date)	02/03/2014	27/03/2015
Maximum snow depth (cm)	253	118
Date of snow cover disappearance	12/07/2014	13/06/2015
Average discharge (median) (m <sup>3</sup> s <sup>-1</sup> )	9.5	5.2

1125 \* Precipitation data are not wind-corrected. Rain vs. snow separation was performed  
1126 following Auer (1974)

1127



1128 Table 2. Topographical characteristics of sub-catchments defined by sampling points.

Sampling point	Description	Catchment area (km <sup>2</sup> )	Glacier cover (%)	Elevation range
T1	Trafoi River	12.18	17	1197 - 3889
T2	Trafoi River	46.72	18.6	1404 - 3889
T3	Trafoi River	51.28	35	1587 - 3469
TT1	Tributary draining Trafoi glacier	4.32	27.1	1587 - 3430
TT2	Small creek	0.05	0	1607 - 2082
TT3	Tributary draining Zirkus/ Circo glacier	6.46	44	1605 - 3888
TSPR1	Spring at the foot of a slope	-	0	1602*
TSPR2	Spring at the foot of a slope	-	0	1601*
S1	Sulden River	130.14	13.6	1109 - 3896
S2	Sulden River	74.61	12.1	1296 - 3896
S3	Sulden River	57.01	15.8	1707 - 3896
S4	Sulden River	45.06	18.6	1838 - 3896
S5	Sulden River	18.91	29.7	1904 - 3896
S6	Sulden River	14.27	38.5	2225 - 3896
ST1	Razoi tributary	6.46	0.6	1619 - 3368
ST2	Zay tributary	11.1	12.8	1866 - 3543
ST3	Rosim tributary	7.3	9.7	1900 - 3542





SSPR1	Spring in the valley bottom near Sulden town	-	0	1841*
SSPR2 - 4	At the base of the rock glacier front	-	0.12**	2614, 2594, 2600*

1129 \* for spring locations, the elevation of the sampling point is given.

1130 \*\* for rock glacier spring locations, the glacier cover refers to the extent of both rock glaciers.

1131

1132 Table 3. Environmental variables derived from the weather station Madritsch/Madriccio at

1133 2825 m a.s.l..

Variable	Unit	Description
$P_{1d}$	mm	Cumulated precipitation of the sampling day
$P_{nd}$		Cumulated precipitation n days prior to sampling day
$T_{max1d}$	°C	Maximum air temperature during the sampling day
$T_{maxnd}$		Maximum air temperature within n days prior to sampling day
$G_{max1d}$	W/m <sup>2</sup>	Maximum global solar radiation during sampling day
$G_{maxnd}$		Maximum global solar radiation within n days prior to sampling day
$\Delta SD_{1d}$	cm	Difference of snow depth measured at the sampling day at 12:00 and the previous day at 12:00, based on 6h averaged snow depth records.
$\Delta SD_{nd}$		Difference of snow depth measured at the sampling day at 12:00 and n days prior the sampling day at 12:00, based on 6h averaged snow depth records.
$D_{Prec1}$	days	Days since last daily cumulated precipitation of > 1mm was measured.
$D_{Prec10}$		Days since last daily cumulated precipitation of > 10mm was measured.
$D_{Prec20}$		Days since last daily cumulated precipitation of > 20mm was measured.



1 Table 4. Statistics of element concentration (in  $\mu\text{g l}^{-1}$ ) from selected stream, tributary and active rock glacier springs in the Sulden catchment  
 2 sampled from March to October 2015. CV: coefficient of variation. VC: variability coefficient (see Eq. 1) with  $SD_{\text{baseflow}}$  (based on samples  
 3 from March, April, and October 2015) and  $SD_{\text{melting}}$  (based on samples from May to September 2015). Note that CV was not calculated for  
 4 SSPR2 – 4 as water samples were available only during summer.

Location	Statistic	Na	Mg	Al	K	Ca	V	Cr	Mn	Fe	Ni	Cu
S1	min	1881.3	12169.1	6.9	1051.2	41497.2	0.2	0.2	1.1	21.1	0.5	1.5
	max	7246.9	19547.1	541.4	2456.0	56508.3	1.8	1.4	62.4	1038.9	3.8	9.1
	mean	3253.5	14625.4	148.7	1657.3	48423.7	0.6	0.6	15.0	292.5	1.3	4.9
	SD	1782.0	2265.3	157.3	487.1	4538.1	0.5	0.3	18.7	300.2	1.0	3.0
S2	CV	0.5	0.2	1.1	0.3	0.1	0.9	0.5	1.2	1.0	0.8	0.6
	VC	0.6	0.3	0.3	1.6	0.5	0.2	0.2	0.1	0.3	0.2	0.8
	min	1968.4	9793.3	6.1	1546.3	43167.9	0.1	0.2	1.1	12.0	0.3	1.3
	max	3334.6	16453.8	743.1	2476.3	73177.3	1.9	1.7	71.0	1513.5	3.8	9.1
	mean	2431.6	12437.2	211.2	1900.9	52361.7	0.6	0.6	18.5	410.7	1.2	3.3
	SD	409.4	2292.5	236.4	299.3	8738.1	0.6	0.5	22.4	467.9	1.1	2.4



	CV	0.2	0.2	1.1	0.2	1.0	0.8	1.2	1.1	0.9	0.7
	VC	2.0	0.2	0.2	0.7	0.1	0.2	0.1	0.2	0.2	0.2
S6	min	1262.6	17458.6	9.0	1042.6	67588.1	0.1	1.5	21.6	0.5	1.5
	max	2277.0	34928.5	799.4	1748.4	166731.5	3.4	104.6	1587.1	6.2	17.0
	mean	1805.6	22862.4	278.4	1362.7	129896.0	1.1	43.1	596.1	2.1	6.5
	SD	339.4	5512.9	321.0	259.4	28165.0	1.2	47.4	670.0	1.9	4.9
	CV	0.2	0.2	1.2	0.2	0.2	1.2	1.1	1.1	0.9	0.8
	VC	0.6	0.2	0.0	1.4	0.5	0.0	0.0	0.1	0.1	0.2
SSPR2-4	min	1768.3	10051.4	9.0	1236.1	76848.5	0.0	1.5	16.7	0.2	0.5
	max	2818.6	29509.5	321.2	2402.5	131149.7	2.5	71.7	492.2	1.5	38.3
	mean	2199.9	17254.4	68.9	2009.0	94611.4	0.4	13.1	127.5	0.7	8.2
	SD	343.3	6935.8	97.8	294.4	21508.4	0.8	22.5	148.5	0.5	11.7
	CV	0.2	0.4	1.4	0.1	0.2	2.2	1.7	1.2	0.7	1.4
T1	min	1125.7	13481.8	6.3	536.9	33044.0	0.2	0.9	13.3	0.3	0.4



	max	3312.9	42197.2	914.7	1470.6	88033.8	4.5	1.8	121.8	1178.5	3.5	22.0
	mean	2078.3	19230.5	139.8	985.9	48369.3	0.8	0.5	19.1	190.2	1.1	5.1
	SD	600.5	8846.6	293.5	302.7	16108.6	1.4	0.5	38.9	374.8	1.0	6.6
	CV	0.3	0.5	2.1	0.3	0.3	1.8	1.0	2.0	2.0	0.9	1.3
	VC	1.3	0.1	0.0	0.8	0.3	0.0	0.3	0.0	0.0	0.2	0.2
TT2	min	321.0	12048.8	4.7	272.8	23873.4	0.1	0.2	0.8	10.4	0.3	0.7
	max	2524.5	20756.5	568.0	1017.1	39335.1	2.0	1.3	57.1	1116.2	2.7	22.2
	mean	1148.1	16898.0	97.0	551.6	32228.7	0.4	0.4	10.2	173.2	0.9	8.0
	SD	727.9	2945.5	179.7	244.1	4615.5	0.6	0.4	17.9	357.5	0.7	7.7
	CV	0.6	0.2	1.9	0.4	0.1	1.5	0.9	1.8	2.1	0.8	1.0
	VC	0.9	0.8	0.1	0.6	0.5	0.1	0.3	0.1	0.1	0.3	0.2

1  
2



1 Table 5. Statistics of element concentration (in  $\mu\text{g l}^{-1}$ ) from selected stream, tributary and active rock glacier springs in the Sulden catchment  
 2 sampled from March to October 2015. CV: coefficient of variation. VC: variability coefficient (see Eq. 1) with  $\text{SD}_{\text{baseflow}}$  (based on samples  
 3 from March, April, and October 2015) and  $\text{SD}_{\text{melting}}$  (based on samples from May to September 2015). Note that CV was not calculated for  
 4 SSPR2 – 4 as water samples were available only during summer.

location	statistics	Zn	As	Se	Rb	Sr	Ag	Cd	Sb	Hg	Pb	U
S1	min	4.1	12.1	0.5	0.0	307.9	0.0	0.0	0.2	0.0	0.4	0.0
	max	23.2	61.1	1.1	2.6	390.5	0.1	0.1	0.5	0.2	7.6	11.3
	mean	9.7	27.0	0.8	1.1	349.8	0.0	0.1	0.3	0.1	2.1	5.1
	SD	5.8	15.5	0.2	1.1	27.2	0.0	0.1	0.1	0.1	2.3	5.2
	CV	0.6	0.6	0.2	1.0	0.1	2.6	1.0	0.4	1.1	1.1	1.0
	VC	0.2	2.6	1.0	0.0	0.7	-	1.0	2.0	0.0	0.1	0.0
S2	min	3.7	15.1	0.4	0.0	334.0	0.0	0.0	0.1	0.0	0.3	0.0
	max	23.8	40.9	0.7	3.4	609.9	0.0	0.1	0.2	0.2	9.4	11.3
	mean	8.5	23.3	0.5	1.6	410.7	0.0	0.0	0.2	0.1	2.7	4.9
	SD	6.4	8.0	0.1	1.6	81.0	0.0	0.0	0.0	0.1	3.4	5.1



	CV	0.7	0.3	0.2	1.0	0.2	-	1.3	0.3	1.1	1.3	1.0
	VC	0.2	2.0	0.5	0.0	0.3	-	1.0	1.0	0.0	0.1	0.0
S6	min	5.6	6.3	0.5	0.0	524.0	0.0	0.0	0.3	0.0	0.4	0.0
	max	40.9	17.0	1.2	1.9	2024.0	0.0	0.2	0.5	0.1	18.1	11.3
	mean	19.1	10.1	0.9	0.7	1380.5	0.0	0.1	0.3	0.0	6.7	4.0
	SD	12.9	4.0	0.2	0.8	463.1	0.0	0.1	0.1	0.0	7.3	4.9
	CV	0.7	0.4	0.2	1.2	0.3	-	0.9	0.2	1.2	1.1	1.2
	VC	0.2	0.1	0.5	0.0	0.5	-	0.5	2.2	0.0	0.0	0.0
SSPR2-4	min	1.5	6.3	0.4	0.0	341.2	0.0	0.0	0.1	0.0	0.2	0.0
	max	49.4	38.0	0.6	2.7	1355.7	0.1	0.4	0.4	0.1	19.8	27.2
	mean	10.7	31.1	0.5	0.9	770.9	0.0	0.1	0.2	0.0	3.1	6.9
	SD	14.8	4.4	0.1	1.0	435.7	0.0	0.1	0.1	0.0	6.3	9.4
	CV	1.4	0.1	0.2	1.1	0.6	2.6	1.4	0.6	1.3	2.0	1.4



T1	min	2.3	7.2	0.6	0.0	220.9	0.0	0.0	0.0	0.2	0.0	0.3	0.0
	max	46.5	64.2	1.4	1.9	478.1	0.0	0.2	0.7	0.2	0.2	18.0	12.5
	mean	10.9	24.5	1.1	0.7	340.1	0.0	0.1	0.4	0.1	0.1	2.9	5.6
	SD	13.6	18.4	0.3	0.7	75.8	0.0	0.1	0.1	0.1	0.1	5.7	5.7
	CV	1.2	0.8	0.2	1.1	0.2	-	1.4	0.4	1.1	1.1	2.0	1.0
	VC	0.1	2.9	0.6	0.0	0.9	-	0.6	2.0	0.0	0.0	0.0	0.0
TT2	min	2.8	0.3	0.5	0.0	149.4	0.0	0.0	0.2	0.2	0.0	0.3	0.0
	max	39.4	1.2	1.5	1.7	384.5	0.5	0.1	0.5	0.5	0.7	9.1	10.6
	mean	9.9	0.7	1.0	0.4	247.5	0.1	0.0	0.3	0.1	0.1	1.8	4.8
	SD	11.4	0.3	0.3	0.5	67.5	0.2	0.0	0.1	0.1	0.2	2.8	4.9
	CV	1.2	0.4	0.3	1.5	0.3	2.6	1.3	0.4	1.8	1.8	1.5	1.0
	VC	0.1	0.3	1.3	0.0	1.2	0.0	1.0	-	0.0	0.0	0.1	0.0



- 1 Table 6. Variability coefficient (VC) for selected locations along the Sulden and Trafoi River
- 2 in 2014 and 2015.

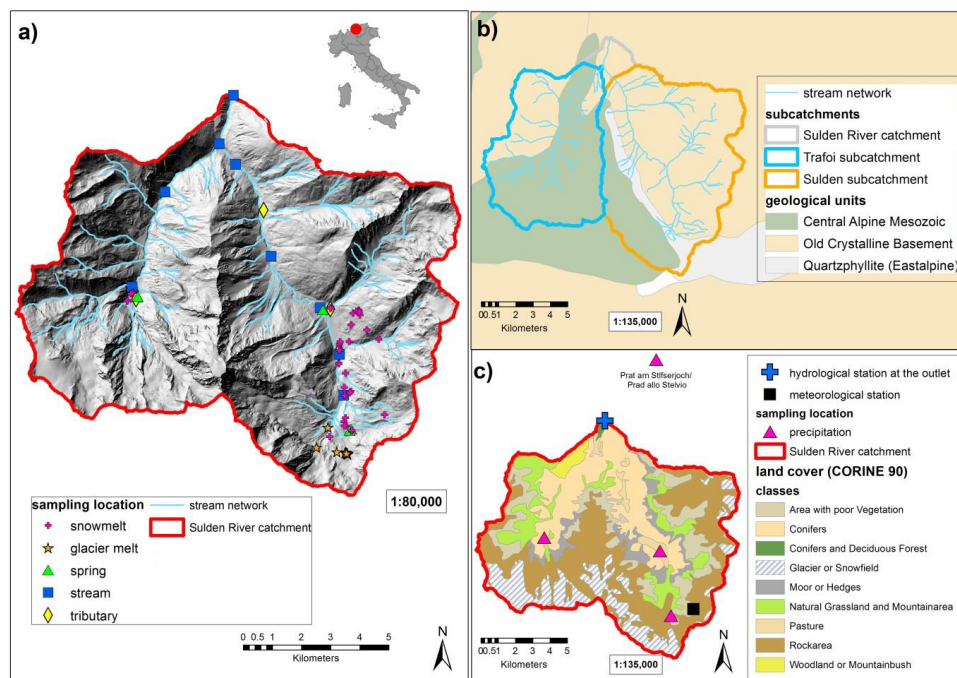
---

Location	River section	VC
	(in km)	
T3	6.529	0.70
T2	2.774	0.85
T1	51	1.09
S6	12.87	0.01
S3	6.417	0.42
S2	2.739	0.35
S1	0	0.77

3

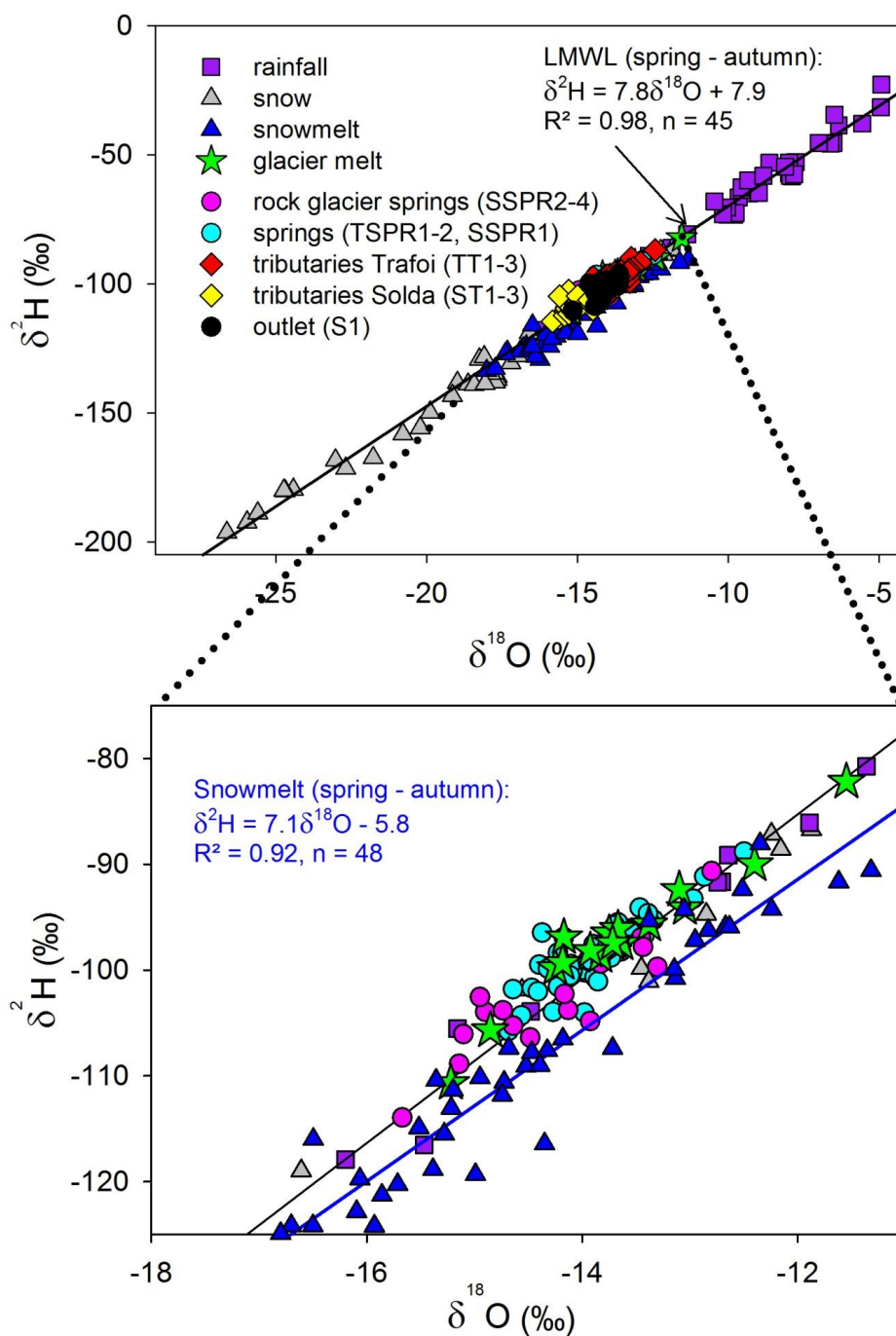
4





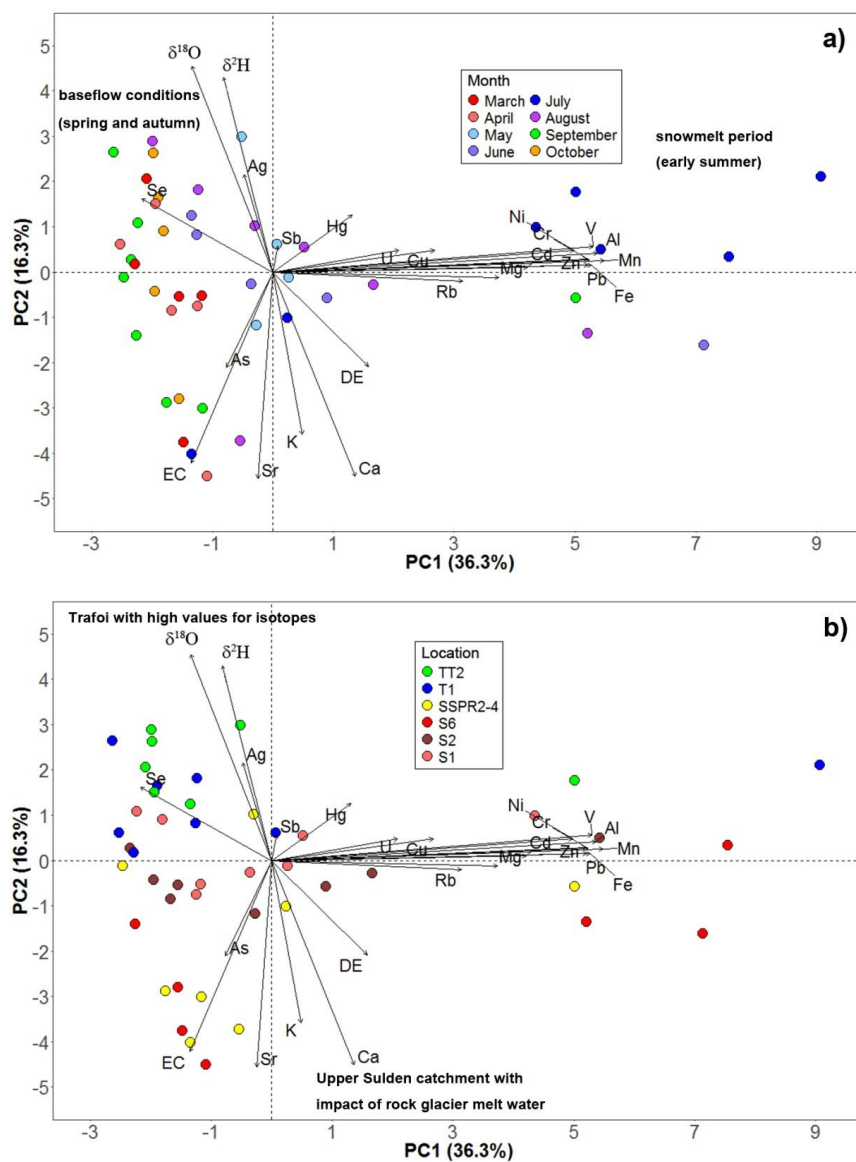
1  
 2  
 3  
 4  
 5  
 6

**Figure 1. Overview of the Sulden catchment with a) sampling point, b) geology, and c) land cover with instrumentation. The meteorological station shown is the Madritsch/Madriccio AWS of the Hydrographic Office (Autonomous Province of Bozen-Bolzano). The glacier extent refers to 2006 (Autonomous Province of Bozen-Bolzano).**





1 **Figure 2.** Meteoric water line of different water sources sampled in the Sulden catchment in 2014 and 2015. The inset  
 2 shows a zoom on rainfall, snow, snowmelt, glacier melt, and spring waters with the regression line of snowmelt  
 3 samples collected from spring to autumn.

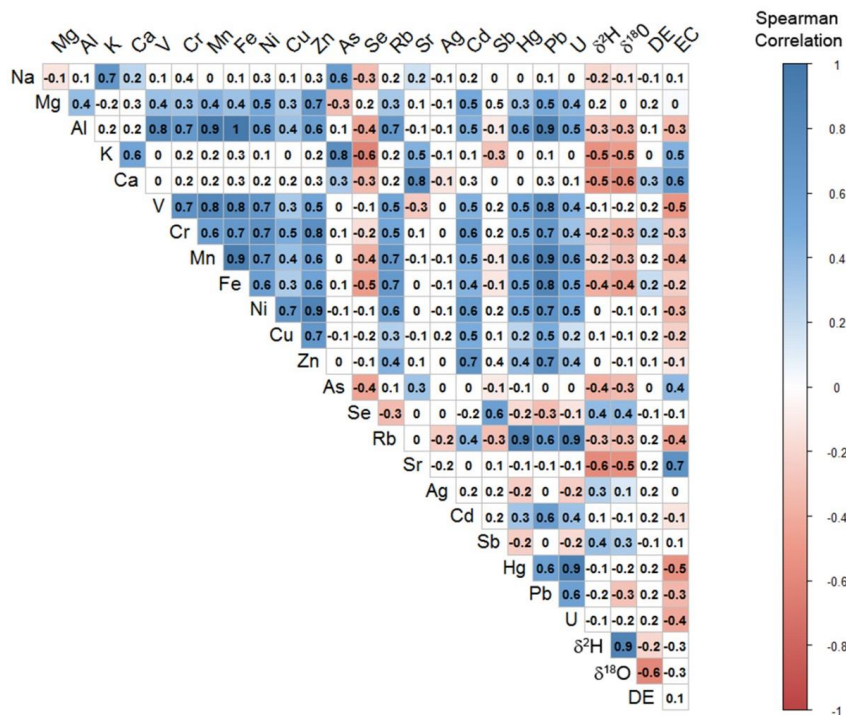


4 **Figure 3.** Principle component analysis of element concentrations of stream water and springs draining a rock glacier  
 5 sampled in the Sulden and Trafoi sub-catchments from March to October 2015. Data based on  $n = 47$  samples are  
 6 shown in groups according to a) the sampling locations and b) the sampling month.  
 7



1

2

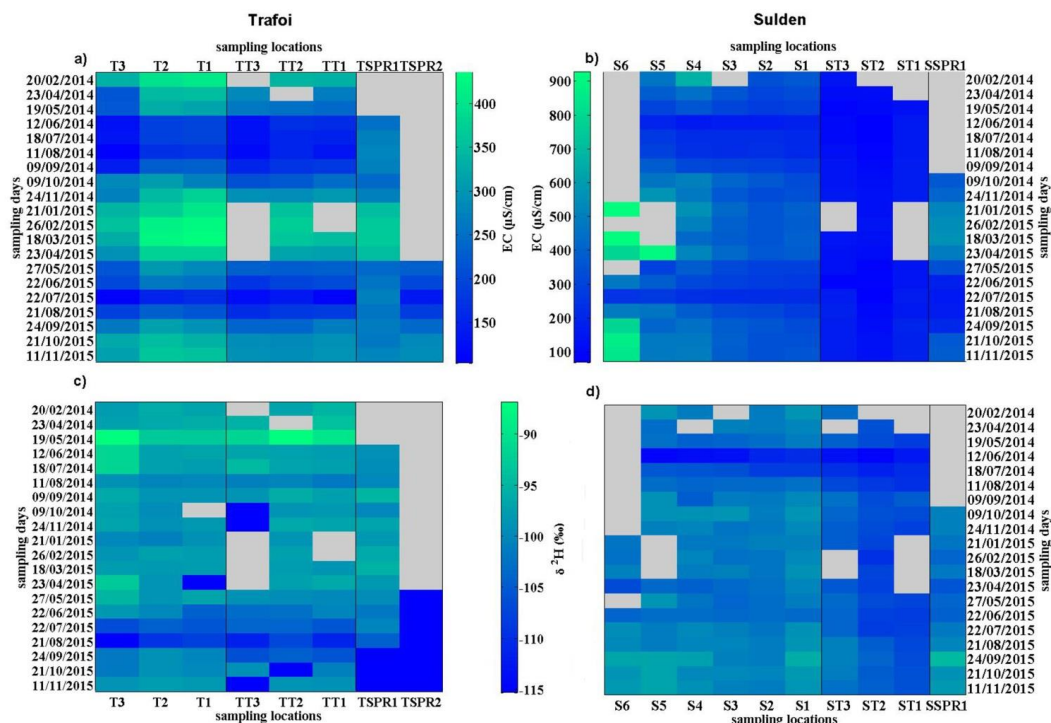


3

4 **Figure 4. Spearman rank correlation matrix of hydrochemical variables. Values are shown for a level of significance  $p$**   
 5 **< 0.05.**

6

7

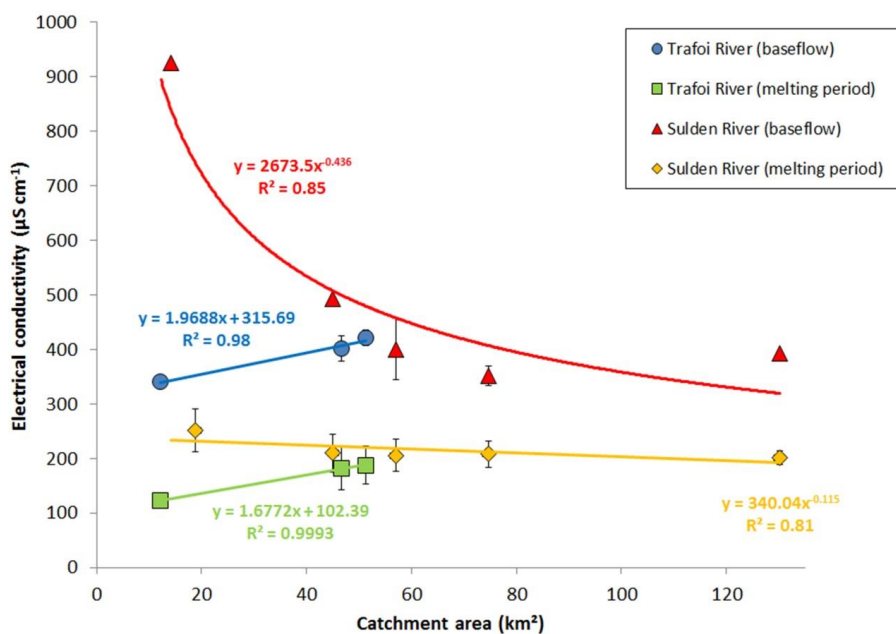


1  
 2  
 3  
 4  
 5  
 6  
 7

Figure 5. Spatial and temporal variability of EC ( $\mu\text{S cm}^{-1}$ ) and  $\delta^2\text{H}$  (‰) at different stream sections, tributaries and springs within the Trafoi sub-catchment (subplot a and c) and the Sulden sub-catchment (subplot b and d) in 2014 and 2015. The heatmaps are grouped into locations at streams, tributaries, and springs. Grey areas refer to missing sample values due to frozen or dried out streams/tributaries or because the sampling location was included later in the sampling scheme.



1

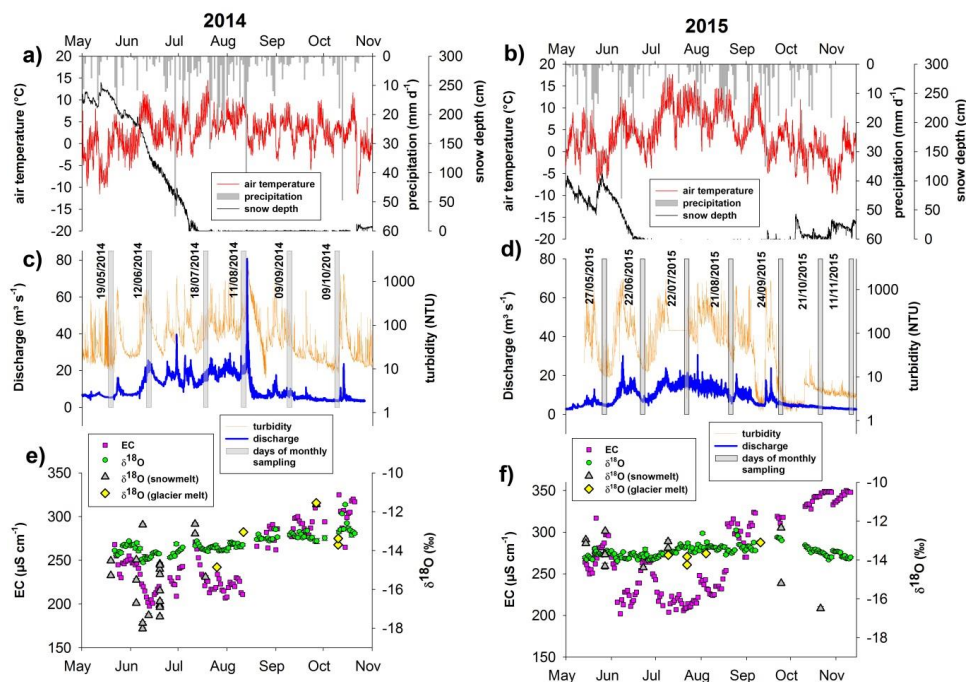


2

3 **Figure 6. Spatial variability of electrical conductivity along the Trafoi and Sulden River against catchment area.**  
4 **Electrical conductivity is averaged for sampling days during baseflow conditions (21/01/2015, 26/02/2015, and**



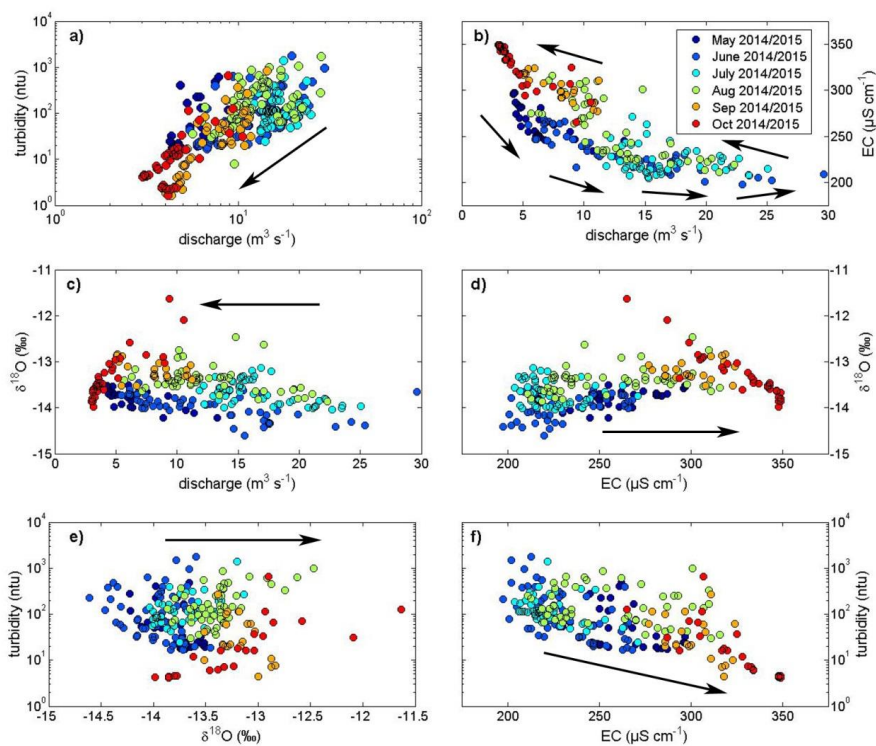
1 18/03/2015) and melt period (12/06/2014, 18/07/2014, 11/08/2014, and 09/09/2014).



2

3 **Figure 7. Time series from 2014 and 2015 of a) and b) precipitation, hourly air temperature and snow depth at the**  
 4 **AWS Madritsch, c) and d) streamflow and turbidity, e) and f) electrical conductivity and  $\delta^{18}\text{O}$  of the stream at the**  
 5 **outlet station Ponte Stelvio and of snowmelt and glacier melt water. Grey shaded bars indicate the date of monthly**  
 6 **sampling carried out in the entire catchment.**

7

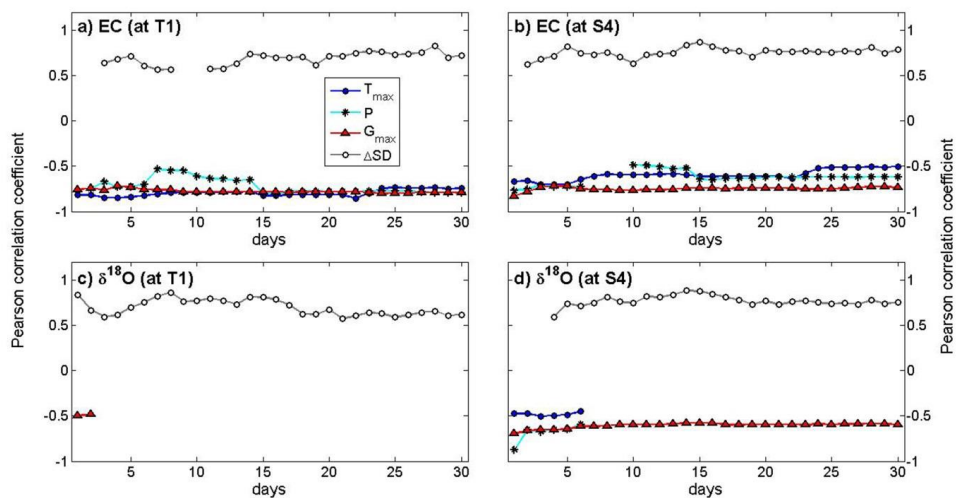


1

2 **Figure 8.** Different combinations of monthly relationships between a) to e) discharge, turbidity and tracers such as EC  
3 and  $\delta^{18}\text{O}$  at Ponte Stelvio in 2014 and 2015. The dataset consists of  $n = 309$  samples. Arrows underline the monthly  
4 pattern.

5

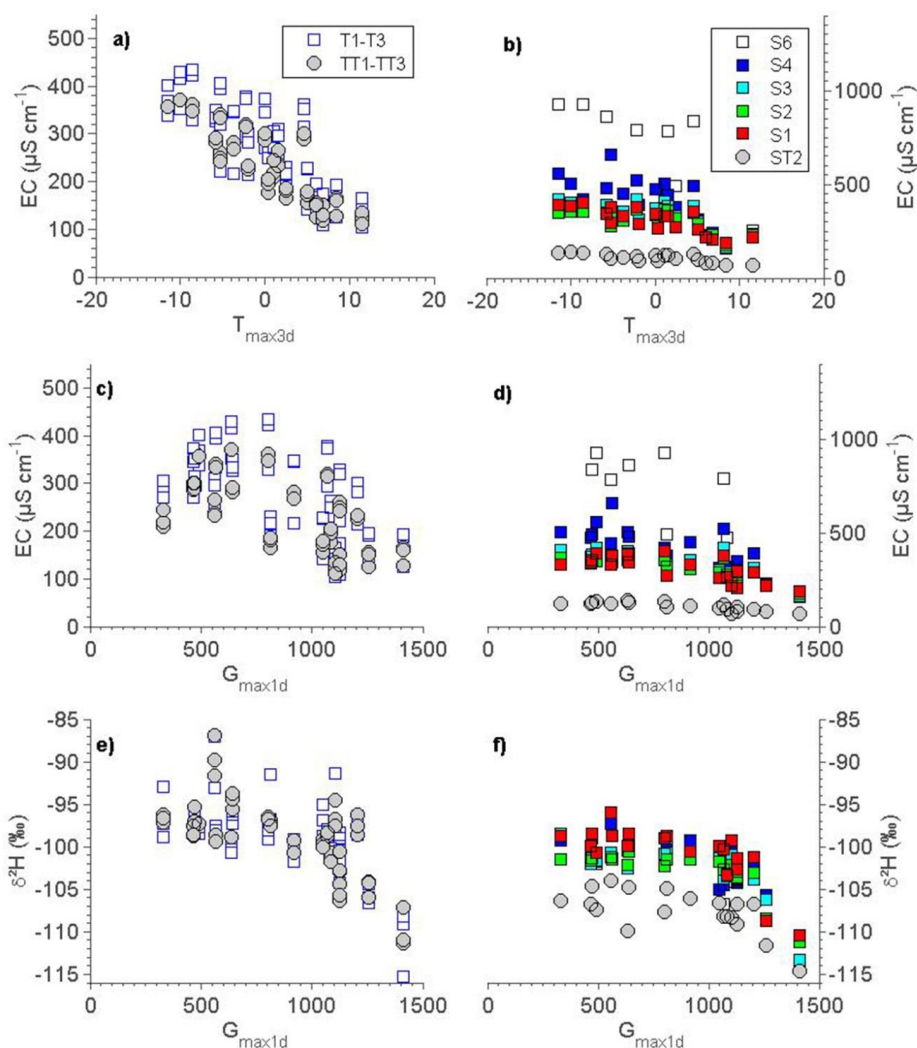




1

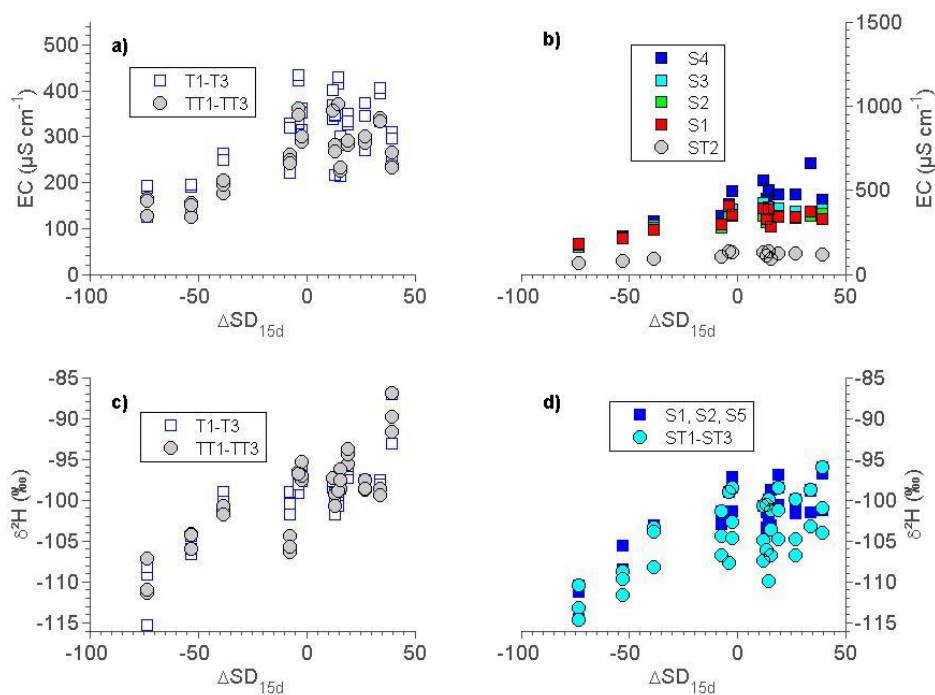
2 **Figure 9.** Temporal sensitivity on the agreement of environmental variables and tracer signatures at the selected  
3 stream locations T1 (Trafoi sub-catchment) and S4 (Sulden sub-catchment). Values are shown for a level of  
4 significance  $p < 0.05$  and missing values refer to non-significant correlations.

5



1

2 **Figure 10.** Major controls of environmental variables on tracer signatures in the study area. Subplots a and b show  
 3 the relationship between electrical conductivity EC and daily maximum air temperature  $T_{\text{max3d}}$  in the Trafoi and  
 4 Sulden River respectively. Subplot c and d show the relationship between electrical conductivity EC and daily  
 5 maximum global solar radiation  $G_{\text{max1d}}$  in the Trafoi and Sulden River, respectively. Subplot e and f show the  
 6 relationship between  $\delta^2\text{H}$  and daily maximum global radiation  $G_{\text{max1d}}$  in the Trafoi and Sulden River, respectively.



1

2 **Figure 11. Major controls of environmental variables on tracer characteristics in the study area. Subplot a and b show**  
3 **the relationship between electrical conductivity EC and 15 days snow depth difference  $\Delta SD_{15d}$  while subplot c and d**  
4 **show the relationship between  $\delta^2H$  and 15 days snow depth difference  $\Delta SD_{15d}$  in the Trafoi and Sulfen River,**  
5 **respectively.**